AIR FLOW BUOYANCY SURROUNDING BUILDINGS IN MALAYSIA

LIAN YEE CHENG

DISSERTATION SUBMITTED IN FULFILMENT OF THE REQUIREMENTS FOR THE DEGREE OF MASTER OF ENGINEERING SCIENCE

FACULTY OF ENGINEERING
UNIVERSITY OF MALAYA
KUALA LUMPUR

2014

AIR FLOW BUOYANCY SURROUNDING BUILDINGS IN MALAYSIA

LIAN YEE CHENG

DISSERTATION SUBMITTED IN FULFILMENT
OF THE REQUIREMENTS FOR THE DEGREE OF
MASTER OF ENGINEERING SCIENCE

FACULTY OF ENGINEERING
UNIVERSITY OF MALAYA
KUALA LUMPUR

2014

UNIVERSITI MALAYA

ORIGINAL LITERARY WORK DECLARATION

Name of Candidate : LIAN YEE CHENG (I.C/Passport No:
Registration/Matric No : KGA100074
Name of Degree : MASTER OF ENGINEERING SCIENCE

Title of Project Paper/Research Report/Dissertation/Thesis ("this Work"):

AIR FLOW BUOYANCY SURROUNDING BUILDINGS IN MALAYSIA

Field of Study:

Air Flow, Buoyancy

I do solemnly and sincerely declare that:

1. I am the sole author/writer of this Work;
2. This Work is original;
3. Any use of any work in which copyright exists was done by way of fair dealing and for permitted purposes and any excerpt or extract from, or reference to or reproduction of any copyright work has been disclosed expressly and sufficiently and the title of the Work and its authorship have been acknowledged in this Work;
4. I do not have any actual knowledge nor do I ought reasonably to know that the making of this work constitutes an infringement of any copyright work;
5. I hereby assign all and every rights in the copyright to this Work to the University of Malaya ("UM"), who henceforth shall be owner of the copyright in this Work and that any reproduction or use in any form or by any means whatsoever is prohibited without the written consent of UM having been first had and obtained;
6. I am fully aware that if in the course of making this Work I have infringed any copyright whether intentionally or otherwise, I may be subject to legal action or any other action as may be determined by UM.

Candidate's Signature Date

Subscribed and solemnly declared before,

Witness's Signature Date

Name:
Designation:

Abstract

In a developing country such as Malaysia, buildings have been built in fast pace. To design a durable building envelope, the air flow around a building plays an important role. The buoyancy is proven as one of the factors induced air flow pattern. The contribution of buoyancy to surrounding air flow of a building in Malaysia was comprehensively investigated in the present research. The objective of the present research is to study the significance of buoyancy in air flow movement with and without present of wind. Future development around the research building was studied as well to examine the effect of the buoyancy to the surrounding air flow. There are three research buildings for present research. The first building is the Malaysia's Energy Commission building. Malaysia's Energy Commission is a green building which has a unique architecture outlook makes it to be called the Diamond Building. Second building is a hospital ward tower of Sarawak International Medical Centre and the third building is Engineering Tower of University Malaya. Outdoor field data such as air velocity, surface temperature and ambient conditions were collected during physical measurement. Three dimensional air flow simulation was then carried out using the Computational Fluid Dynamics (CFD) software ANSYS. Qualitative and quantitative analyses of the simulation results have been carried out to investigate the influence of the buoyancy effect on the air flow surrounding buildings. The result shows that the air flow surrounding the green building has a maximum velocity of 0.69 ms^{-1}, hospital ward tower is 0.25ms^{-1} and engineering tower is 0.19ms^{-1} which is dominated by the buoyancy effect when no wind is present. The buoyancy strength is quantified by a dimensionless number, Archimedes number. If natural wind is present, the buoyancy effect is negligible.

Abstrak

Di negara yang sedang membangun seperti Malaysia, bangunan telah dibina dengan cepat. Untuk mereka bentuk bangunan yang tahan lama, aliran udara di sekitar bangunan memainkan peranan yang penting. Keapungan dibukti sebagai salah satu faktor yang menyebabkan corak aliran udara. Sumbangan keapungan kepada sekitar aliran udara sebuah bangunan di Malaysia disiasat secara komprehensif dalam kajian ini. Objektif adalah untuk mengkaji kepentingan daya apung dalam aliran udara dengan dan tanpa hadir angin. Pembangunan masa depan di sekitar bangunan penyelidikan juga dikaji untuk menguji pengaruh keapungan untuk aliran udara sekeliling. Ada tiga bangunan penyelidikan untuk kajian ini, pertama adalah bangunan Suruhanjaya Tenaga Malaysia, kedua adalah menara wad hospital dan ketiga adalah Menara Kejuruteraan Malaya Universiti. Suruhanjaya Tenaga Malaysia adalah sebuah bangunan hijau yang mempunyai seni bina berlainan unik membuatnya yang dikenali sebagai Bangunan Diamond. Data lapangan luar seperti halaju udara , keadaan ambien dan suhu permukaan dikumpulkan selama pengukuran fizikal. Tiga dimensi simulasi aliran udara dilakukan dengan menggunakan Komputasi Dinamik Bendalir (CFD) perisian ANSYS. Analisis kualitatif dan kuantitatif hasil simulasi telah dilakukan untuk menyiasat pengaruh kesan keapungan pada corak aliran udara. Hasil kajian menunjukkan bahawa aliran udara yang mengelilingi bangunan hijau mempunyai halaju maksimum 0.69 ms^{-1} dan untuk menara wad hospital adalah 0.25ms^{-1} dan menara kejuruteraan adalah 0.19ms^{-1} didominasi oleh kesan keapungan apabila tiada angin hadir. Jika angin semula jadi hadir, kesan keapungan diabaikan.

Acknowledgements

I would like to deliver my deepest appreciation to my supervisor, Associate Professor Ir. Dr. Yau Yat Huang for his guidance. Nevertheless, I would like to appreciate Mr Ding Lai Chet, Mr Tommy Chang Chee Pang and Mr Kong Keen Kuan, for their help and suggestions throughout the candidature.

TABLE OF CONTENTS

LIST OF FIGURES

LIST OF TABLES

LIST OF SYMBOLS AND ABBREVIATIONS

Ar	Archimedes number
CFD	Computational Fluid Dynamics
Gr	Grashof Number
g	Gravitational acceleration, ms^{-2}
H	Height of building, m
h	representative mesh size, m
k	turbulent energy
L	Characteristic length, m
Re	Reynolds number
$T- T_{\infty}$	Temperature difference, ^{o}C
U	Velocity, ms^{-1}
U^*_{ABL}	Atmospheric boundary layer friction velocity, ms^{-1}
U_h	Specified velocity, ms^{-1}
W	Width, m
P	Static pressure, Pa
r	Diffusion coefficient, $m^2\ s^{-1}$
$\check{T}$	Thermal fluctuation
∇^2	Differential operator

Greek symbol

σ	Prandtl number of fluid
β	Coefficient of thermal expansion, K^{-1}
ε	Rate of dissipation, m^2s^{-3}
κ	Karman constant
ρ	Air Density, $kg\ m^{-3}$
μ	Fluid dynamic viscosity, $kg\ m^{-1}s^{-1}$
ν	Kinematics viscosity, $m^2\ s^{-1}$

CHAPTER 1
INTRODUCTION

1.0 Introduction

1.1 Background

Building envelope is important issue in sustainable development. Our outdoor conditions are getting worse due to the green house effect. Air flow is among the factors in designing building envelope. In order to design a good building envelope, lots of outdoor environment data are required. Malaysia is a developing country in which building is built in a very massive rate especially in capital, with different architectural designs, heights and shapes. Outdoor environment conditions are differ between city and a rural area with building in city are dense while in rural area are scattered. Indoor thermal comfort is more emphasized when designing a building, but the indoor is in relation with outdoor condition as well. There are many studies on the outdoor airflow surrounding building, but these studies ignore the buoyancy effect. There are studies on airflow induced by buoyancy inside a building, yet there are insufficient studies and data regarding outdoor buoyancy effect. Outdoor environment condition is hardly to be constant due to natural phenomena, hence the data can be collected to predict a trend of the airflow. Excessive development and increase of high rise buildings will finally lead to the worsening of the urban outdoor thermal environment. In Malaysia, land price is getting higher because the area available for development is getting less. So more and more high rise buildings are built. High rise building built one after another has caused the area becomes denser and the effect of this phenomena to the surrounding airflow is unknown. The airflow of a building located in a densely built area and a scattered built area is different because in rural area airflow is greatly affected by environment airflow because there is less obstacles. Understanding of a

building's outdoor environment condition is very important as it contributes in building's energy usage.

1.2 Scope of work

In this study, air flow characteristic surrounding three buildings in Malaysia which consist of one green building and two conventional building has been investigated. Current work includes on-site measurement of air velocity, surface temperature of building and ground as well as ambient temperature. The buildings are modeled and the air flow is predicted using commercial Computational Fluid Dynamics (CFD) software ANSYS Fluent. The results from the numerical results were further analyzed in term of buoyancy effect on air flow structure.

1.3 Objectives of the study

The overall objective of this study is to investigate the buoyancy effect to outdoor air flow structure around buildings in Malaysia. The objectives are:

1. To perform fieldwork measurement such as velocity and temperature of outdoor air flow at Suruhanjaya Tenaga (Green Building), Ward Tower of Sarawak General Hospital Heart Centre (Conventional Building) and Engineering Tower of University Malaya (Conventional Building).
2. To carry out CFD investigation on buoyancy effect for outdoor airflow structure surrounding these three buildings.

This overall objective will be achieved by accomplishing the following itemized technical objectives.

1. Field measurements of air velocity, ambient temperature, ground and building wall surface temperature to establish the boundary conditions needed for CFD modeling.
2. Quantitative assessment and verification of the CFD simulations by comparison with fieldwork measurement.

1.4 Significance of the study

It has been a popular study on outdoor airflow, but lack of study on buoyancy effect. This research provides a case study based on actual outdoor environment in Malaysia and provides insight of buoyancy effect for outdoor airflow surrounding buildings.

1.5 Limitations of the study

1. The lack of full scale laboratory restricted the scope of comparison (verification) between predicted and actual air distribution.
2. The scope of current study is focused on specific timeframe which is from 11.00am to 1.00pm, with certain period of time in a year, other timeframe will have different result from this study.
3. The scope of current study is focused on particular environment condition, so the result might be different with different environment.

1.6 Outline

This research dissertation is divided into several main chapters.

Chapter 1 points out the overview, background, scope of work, objectives of present study, significance and limitations of the study.

Chapter 2 outlines the literature review covered in this research topic, known as air buoyancy, air flow around building, computational fluid dynamic and tropical climate.

Chapter 3 emphasizes on the methodology to fulfill the objectives of this research.

Chapter 4 studies and analyzes the Computational Fluid Dynamics result of buoyancy on airflow surrounding a green building, Suruhanjaya Tenaga.

Chapter 5 studies and analyzes the Computational Fluid Dynamics result of buoyancy on airflow surrounding a hospital ward tower, Sarawak International Medical Centre.

Chapter 6 studies the fieldwork and Computational Fluid Dynamics of buoyancy on airflow surrounding Engineering Tower of University Malaya.

Chapter 7 outlines the dissertation with summary and future recommendation.

CHAPTER 2

LITERATURE REVIEW

2.0 Literature Review

Diminishing energy resources, environmental awareness and global warming had made sustainable development more widely recognized. New approach, design and strategies for sustainable building development had been emphasized. It is often heard that environmental rating of a building is pointing at buildings with comfortable indoor environment that consume less energy to operate and produce little pollution during operation. It is noticed over the last two decades a real trend to improve the quality of both buildings and their environment. A growing number of Green Buildings made this trend noticeable (Garde-Bentaleb et al., 2002).

Cities in tropical countries are falling short of sustaining outdoor environment with rapid urbanization. Urbanization is overwhelming and guides the development of every walk of life in the whole world. It is inevitable in developing countries due to high population (Lu et al., 2007). This will lead to climate changes in long run which further diminishing urban energy resources. A desirable outdoor environment has a good implication in building envelope's design. For free running buildings such as the natural ventilated building, comfortable ambient climate leads to comfortable indoor environment. Sustainability of urban environment can be achieved by defining outdoor environment condition comfort. Indoor environment had a significant relationship with outdoor spaces in the perception of comfort. Due to uncomfortable outdoor conditions, building's indoor comfort environment is highly demanded. Promoting the construction of green building by ensuring a

comfortable urban micro climate can be regarded as a way in supporting the practices of sustainable development. The environmental factor has the significant impact especially in the natural ventilated building, the indoor comfort is expanded to include the outdoor effect. Therefore, in the perception of comfortable indoor environment, it is considered that outdoor environment has more direct influence (Ahmed, 2003).

Energy consumption of an urban building can be burdened by rapid urbanization. The actual outdoor environment such as air temperature, wind velocity and solar radiation can be modified by the design of outdoor spaces (Givoni et al., 2003). Due to outdoor discomfort, which mainly thermal discomfort, people tend to spend time in indoor. It is important to study the factors in order to improve outdoor comfort conditions.

Green building practices aim to reduce the environmental impact of building. Driven by environmental needs, Green Building Index (GBI) was jointly founded and developed by Pertubuhan Akitek Malaysia (PAM) and the Association of Consulting Engineers Malaysia (ACEM) in 2009. GBI(M) is a profession driven initiative to lead the property industry towards becoming more environment-friendly. From its inception GBI has received the full support of Malaysia's building and property players. It is intended to promote sustainability in the built environment and raise awareness among Developers, Architects, Engineers, Planners, Designers, Contractors and the Public about environmental issues.

2.1 Air buoyancy

The influence of heat on air flow and its vertical transport capabilities in canyon is studied by differential heating of the canyon surface which is $5^{o}C$ higher relative to the other. Vertical flow is observed due to buoyancy flux increases upward advection along the wall when the leeward wall is warmer than air. The cell is well centered within canyon when the

ground is warmer than air. When the windward wall is warmer than air, an upward buoyancy flux opposes the downward advection flux along this wall and the flow structure is divided into two contra rotating cells (Sini et al., 1996).

In a naturally ventilated enclosure experiment, the mean velocity vector of outflow and inflow through upper vent are inclined to the horizontal plane due to the effect of buoyancy. When the temperature difference between inside and outside is relatively small, the vectors become more parallel to the horizontal plane (Tanny et al., 2008). In a solar chimney, solar radiation passing through a transparent wall is absorbed by the other walls of vertical channel. The air inside the channel warms up and a natural flow is established within the channel due to the buoyancy effect (Arce et al., 2009).

In a study of influence of buoyancy on turbulent flow which affect the heat transfer. Effectiveness of heat transfer was modified by the distortion of the mean flow due to the influence of buoyancy and the effect that this had on turbulence production and turbulent diffusion of heat (Wang et al., 2004).

There are studies about the buoyancy affected airflow patterns at different wall temperature. Steady and incompressible flow has been considered. Navier stokes equation and energy equation in 2-dimensional rectangular Cartesian coordinates have been numerically solved using control volume method. Boussinesq approximation has been used for buoyancy force (Tripathi and Moulic, 2007).

Relationship between surface temperatures to buoyancy effect is investigating through Grashof number. Grashof number is a dimensionless number which is the ratio of buoyancy force to viscous force acting on fluid. Buoyancy effect results in natural tendency of a substance to migrate due to some driving force. Buoyancy force caused by a temperature

gradient, as the fluid would be at rest in the absence of temperature variations. The Grashof number is analogous to the Reynolds number if flow has external driving force. The ratio of Gr/Re^2 is Archimedes number, which represents the ratio of buoyancy force and inertia force. If the value is greater than 1, the buoyancy effect is significant and if value is smaller than 1, external force dominates the fluid flow. The larger the temperature differences between the fluid adjacent to a hot or cold surface and the fluid away from it, the larger the buoyancy force.

$$Gr = \frac{g\beta\ (T_s - T_\infty)L^3}{\nu^2} \quad (1)$$

$$Ar = \frac{Gr}{Re^2} \quad (2)$$

2.2 Air flow around building

2.2.1 Air flow due temperature

Understanding the effect of urban geometry is an important issue when doing urban planning and building design in order to plan a more sustainable city. A research on investigation of urban geometry effect which is characterized by the plan area ratio and building aspect ratio as well as heterogeneity of building heights is conducted (Abd Razak et al., 2013).

Before performing the urban residential district planning, analyses of the design parameters is crucial to find out the scientific and accurate data. This can improve the outdoor environment around the building cluster and reduce the energy consumption during building operation period (Tang et al., 2012).

Different building designs such as building width, height, and shape ,as well as the orientation of streets in proximity to the built areas, can have a major effect on wind velocity at inlet surfaces of buildings (Rizk and Henze, 2010).

High rise building has a main disadvantage on aspects of blocking wind field. The decreasing wind speed results in the accumulation of the air-conditioning heat revolving region where sunshine cannot rip into (Lu et al., 2007). When the air flow is blocked by the building obstacles, especially upwind obstacles, turbulence is generated. As the flow advance from upstream to downstream, the magnitude and turbulence profile are not greatly affected by the input turbulence profiles (An et al., 2013).

An experimental investigation was carried out to determine the effect of trees on buildings micro-climate in and around two typical buildings located on a university campus. Indoor air temperature, outdoor air temperature and wall temperature were measured, while ancillary wind and solar radiation data were collected from the campus meteorological station. Air temperatures were higher throughout the study period inside the un-shaded building. Outdoor temperature was analyzed to understand the effect of solar radiation and wind speed. The diurnal variation of wall temperature is also considered while energy consumption for cooling in both buildings was compared (Morakinyo et al., 2013).

Speed and direction of the wind vary considerably outdoors, and especially in urban areas. Preferably three dimensional measurements (measuring horizontal as well as vertical wind speeds) should be performed since the wind direction is very irregular. The instruments need to have a quick response time and sufficient accuracy. A temperature probe exposed to solar radiation may overestimate the air temperature by several degrees Celsius, according to existing standards. Hence proper shielding of the probes to minimize radioactive exchange between the instrument an its surroundings.

A number of field experimental procedures were performed in an urban street canyon, aiming at the investigation of the thermal and airflow characteristics during hot weather condition (Niachou et al., 2008a, Assimakopoulos et al., 2006, Niachou et al., 2008b, Georgakis & Santamouris, 2006). Canyon's relative geometry will determine the characteristics of airflow. (Nakamura and Oke, 1988) . Researchers are interested in the vertical structure of the airflow in the canyon such as the number and intensity of vortices induced. Thus the net effect seems to indicate that when the prospect H/W increases, the canyon becomes more isolated from the air above in terms of air exchanges and ventilation (Eliasson et al., 2006).

2.3 Computational Fluid Dynamic

2.3.1 Background

Computer simulation has been applied in engineering research for decades. The trend of CFD usage is increasing every year (Oberkampf and Trucano, 2002). Computational Fluid Dynamics has been recognized for its effectiveness in assisting of indoor and outdoor building design. It has been well acknowledged in HVAC field and environmental predictions (Zhang et al., 2010).

There were many computational models developed to investigate various cases of indoor and outdoor of buildings. These models are used to analyze the characteristic of wind environment during the design process. There are many advantages of using CFD during design stage compared to other approaches. CFD can be used to analyze a future building design, which is currently unavailable. It also provides a valuable insight for some complex configuration which theoretical experiment is hardly to conduct. In experiment for the big

dimension configuration, it is usually done by reducing the scale and carry out in wind tunnel. Other than that, reduced scale wind tunnel experiment needed to verify the similarity requirements. CFD allowed full scale control on all the parameters, including meteorological conditions and it is able to provide all the detailed information at every point of the computational domain, which means the whole field data. CFD also allowed easily evaluation of different alternative design, especially when the different configurations are embedded in the same computational domain. CFD simulations can be run at full scale that makes it not restrain of the similarity requirements (B. Blocken et al., 2012). CFD modeling and simulation results can have a great impact on engineering field.

There are plenty of CFD software in the market, ANSYS FLUENT is among the popular. It could analyze fluid flow and heat transfer with a complex transient reacting flow. It is a fully featured fluid dynamic solution for flow modeling.

CFD has been used to investigate the mean flow patterns within different block arrays configuration with varied building height. This investigation has contributed to the determination of urban aerodynamic parameters under different geometric conditions (Jiang et al., 2008). Air flows are visualized in laboratories or modeled by CFD numerical calculations (Sini et al., 1996). There are important techniques in using CFD to simulate appropriate prediction of wind environment, in the aspect of computational domain, grid discretization, boundary condition and etc (Tominaga et al., 2008).

The main concern of using CFD is the reliability and accuracy of its result (Hooff and Blocken, 2010). The accuracy of results of computational fluid dynamics simulations strongly depends on the turbulence model applied when the Reynolds Averaged Navier Stokes approach is used. (Van Maele and Merci, 2006).

2.3.2 Turbulence model

Choices of the basic equation have the largest impact on the modeling errors and uncertainties. First it has to be decided whether the application requires an unsteady or a steady treatment. Choice of turbulence models can influence the accuracy and reliability of a CFD simulation (Tominaga et al., 2008). Turbulent flow model has better compromise result then laminar flow model when comparing the predicted and measured value. Yet, there is no single turbulent flow model that is suitable to solve all kind of air flow pattern. Improper selection of turbulence model may result in inaccurate air flow result (Chen, 2009).

The Reynolds-averaged Navier-Stokes equations (RANS equations) are time-averaged equations of motion for fluid flow. The RANS equations are mainly used to solve turbulent flows. RANS-based k-epsilon turbulence models divided into three categories, standard k-epsilon model, realizable k-epsilon model and RNG k-epsilon model. The standard k-ε model is a mature turbulence model that had been used and validated extensively by other researchers (van Hooff and Blocken, 2013). In the model, there are two quantities: k, the turbulent kinetic energy and ε, the rate at which the kinetic energy dissipated. The computational simulation utilizing the standard k-ε turbulent model with isothermal condition agrees closely with the measurements taken from the field investigation (Rajapaksha et al., 2003).

3D unsteady Reynolds-averaged Navier-Stokes (RANS) CFD simulations has been used in the study of wind flow and indoor air flow in a large semi-enclosed stadium model. (van Hooff and Blocken, 2013). There is a study of sensitivity on inflow turbulence profile to downstream wind velocity profile with street array of urban environment. Realizable k-ε turbulence model is used to model the wind environment (An et al., 2013). In a wind flow

simulation around building, realizable k-ε turbulence model is chosen due to its general good performance (van Hooff and Blocken, 2013). A study of air flow around buildings proposed usage of RANS, instead of large eddy simulations (LES). LES is difficult in practical analysis due it require huge number grids (Tominaga et al., 2008). In a wind tunnel experiment for 2-D ventilated greenhouse, RNG model has shown a better air flow pattern compared to other SKE model (Tong et al., 2013). Other than that, RNG models also showed a better result compared to other model in air temperature and air velocity measurement of a livestock building and greenhouse (Rohdin and Moshfegh, 2007). RNG model is more suitable in solving weak or low velocity air flow than SKE, RKE, SKW or the KWSST models (Coussirat et al., 2008).

It is recommended double precision should be used due to the result precision. Single precision can be used if the target parameter and variable result demonstrated by it is not strongly affected (Franke et al., 2011). In a research, pressure-velocity coupling is taken care of by the SIMPLEC algorithm, pressure interpolation is standard and second-order discretisation schemes are used for both the convection terms and the viscous terms of the governing equations (van Hooff and Blocken, 2013).

2.3.3 Domain size and geometrical modeling

Normally the distribution of buildings has the greatest impact on wind flow patterns. Secondary factors influence wind flow in the urban area include vegetation, topography and surface characteristics, such as roads, grass and ground. The research building should be located in the middle of the domain. The central area of interest should be reproduced with as much detail as possible. Other than the research building, all the obstacles that could affect the airflow should be contained in the computational geometry (Blocken et al., 2007,

Tominaga et al., 2008). In an actual urban area, the interested region should be modeled, generally 2H radius from the interested building. It is suggested that at least one additional street in each direction of target building be clearly reproduced (Tominaga et al., 2008). For the buildings that are 2H further from interest location, from the outer edge of interest region to boundary, it can be modeled implicitly, which will specify appropriate surface roughness boundary condition (Bert Blocken et al., 2007). It should be noted that there is a possibility of unrealistic results if the computational region is expanded without representation of surroundings

Computational domain size in vertical and lateral is determined by the blockage ratio, which is recommended to be below 3%. Blockage is defined as the ratio of the projected area of the building in flow direction to the free cross section of the computational domain. From wind tunnel experiment, the lateral and top boundary is suggested to be 5H away from the target building, which H is the height of target building. Height of the domain can also be determined according to boundary layer height of surrounding terrain category (Tominaga et al., 2008). For vertical extension of the domain, top of computational domain should be at least 5H above the roof of the building, where H is the building height. The inlet boundary is suggested be set according to upwind area which usually is 5H while outflow boundary is at least 10H away from target building to allow for flow re-development behind the wake region.

2.3.4 Meshing

There are two types of discretisation method of computational grid for equation solving, Finite Element and Spectral. Computational results are highly dependent on discretisation method. The grid has to be designed in appropriate way to minimize the errors introduced

by it. The grid should be able to capture vortices and shear layer, so resolution should be fine and good quality. Hence, grid compression or stretching should be small in the high gradient region. It is suggested that the expansion ratio between 2 grids should be below 1.3. However, mesh generation is complicated and time consuming process especially for complex geometry (Zhang et al., 2010). Finer grid will require longer simulation times and computing resources, but give a more accurate result. Thus a compromise is needed between the simulation accuracy and time (Tong et al., 2013).

There are three categories of 2D meshes, which are triangle, quadrilateral and hybrid meshes. Triangle elements can easily cover a complex geometry, but quadrilateral element provides more accurate simulation result. For 3D meshes, hexahedral or prismatic elements near solid boundaries are preferable, with the element face perpendicular to the boundary. It is suggested that the element near wall should orthogonal to the wall (Tominaga et al., 2008). This grid can be easily generated by grid generation technique for complex geometry (van Hooff and Blocken, 2010). The grid resolution should refer to grid convergence analysis to investigate the grid sensitivity (Tominaga et al., 2008). For grid convergence studies, using the grid convergence index (GCI) is recommended.

2.3.5 Boundary condition and setting

Choices of boundary condition are very crucial. The boundary conditions represent the influence of the surroundings that have been cut off by the computational domain. As they determine to a large extent the solution inside the computational domain, their proper choice is very important. Often, however these boundary conditions are not fully known. Therefore the boundaries of the computational domain should be far enough away from the region of interest to not contaminate the solution there with the approximate boundary

conditions. Boundary condition such as inflow, outflow, top and lateral boundary should be consistent, that will not yield unintended stream wise.(Blocken et al., 2007; Hargreaves and Wright, 2007).

For wall boundary condition, it is suggested walls with no slip boundary is used. Wall functions are applied to compute wall shear stress, which is computed from logarithmic velocity profile between wall and the first element node normal with wall direction. For urban areas, rough wall are chosen. In meteorological codes, the roughness is included by the hydrodynamic roughness length z_0.

For outflow boundary condition, it is suggested using open boundary condition, where most of the fluid leaves the domain. The open boundary is either outflow or constant static pressure boundary conditions. This boundary should be ideally far enough away from the built area to avoid any fluid entering into the computational domain through this boundary. Flow entering the domain through the outflow boundary should be avoided as this can negatively impact on the convergence of the solution or even allow no converged solution to be reached at all.

For top boundary condition, the choice is very important for sustaining equilibrium boundary layer profiles. Therefore prescription of a constant shear stress at the top, corresponding to the inflow profiles, is recommended to prevent a horizontal change from the inflow profiles.

For inflow boundary conditions, at the inflow an equilibrium boundary layer is usually prescribed. The mean velocity profile is usually obtained from the logarithmic profile corresponding to the upwind terrain via the roughness length z_0 is used to determine the wind speed at the reference height. For steady RANS simulation, the mean velocity profile

and information about the turbulence quantities is required. Their profile can be obtained from the assumption of an equilibrium boundary layer. The effect of changes in wind direction with height is to be included in the model by properly selecting the incoming flow profile.

The unintended differences between inlet profiles and incident profiles (the horizontal homogeneity problem) can be detrimental for the success of CFD simulations given that even minor changes to the incident flow profiles can cause significant changes in the flow field. Indeed sensitivity studies have indicated the important influence of the shape of the vertical incident flow profiles on the simulation results of flow around buildings (Gao and Chow, 2005).

Best practice guidelines provide procedures for the model user so as to estimate and reduce errors and uncertainties in the results of a numerical simulation. There are structures indicating a sequential way to conduct a numerical simulation, it should be stressed at this point that there is interdependence among these steps. The recommended strategies refer to ideal situations which might not be encountered in all simulations due to resource limitations or failure of the strategies in principle.

First order discretisation schemes should not be used due to the associated large amount of numerical diffusion at least formally second order accurate discretisation schemes should be used. Theses however impose stronger demands on the quality of the computational grid, computational grids with lower quality cells, such as tetrahedral cells, might show convergence difficulties when combined with higher order discretisation schemes.

Iterative convergence should be monitored and should not be terminated without assurance that further iterations will not yield substantial changes in the flow variables of the interest (Tominaga et al., 2008).

A boundary layer is the layer of fluid in the immediate vicinity of a bounding surface where the effects of viscosity are significant. There are three types of near wall treatment, standard, non-equilibrium and enhance.

For outdoor environment flow, there are two categories of flow, High Reynolds and Low Reynolds. Walls are significantly affecting the turbulent flow, because of its no slip condition, which the air velocity at the wall surface is zero, thus the shear stress will go to maximum. The near wall region can be divided into three layers, there are viscous sub-layer, buffer layer and fully turbulent layer. Viscous sub-layer is a layer flow is nearly laminar. Buffer layer is the transition layer between the laminar flow to the fully developed turbulent flow. Fully turbulent layer is the layer with fully developed turbulent flow, which is also call as log-law layer (Zhang et al., 2010). Near wall treatment is the set of near wall modeling assumptions for turbulence model. Wall functions are sets of semi empirical functions used to solve the flow in the near wall region. Each region has a different effect on turbulence and particular care must be taken to the y^+ position of the first cell in the boundary layer (ANSYS, 2009a, 2009b). Near wall treatment is taken care of using wall functions.

Air flow simulation results depend on a good prediction of near wall turbulence. In this paper a comparative study between different near wall treatments is presented. In each case, suitable meshes with adequate position for the first near-wall node are needed. Reynold-averaged Navier-stokes (RANS) turbulent models (such as k-e models) are still widely used

for engineering applications because of their relatively simplicity and robustness. However, these models depend on adequate near-wall treatments.

Atmospheric Boundary Layer (ABL) is the layer closest to the ground, contact with the ground surface, land or sea. The friction exerted by the wind against the ground surface; this friction causes the wind to be sheared and creates turbulence. When the ABL is said to be neutral, we expect a logarithmic velocity profile u(z) characterized by the friction velocity u_* and the roughness height z_o.

Accurate simulation of ABL flow in the computational domain is imperative to obtain accurate and reliable predictions of the related atmospheric processes (Wieringa, 1992). Simulation of a horizontally homogenous ABL is very important in a computational domain. It indicates that this profile is maintained from upstream to downstream for an empty domain, without interference of vertical streamwise gradients. At the domain upstream, the flow can be divided into three types, inlet flow, approach flow and incident flow. Horizontal homogeneity implies that the inlet profiles, the approach flow profiles and the incident profiles are the same (Blocken et al., 2007). These profiles should be representative of the roughness characteristics of that part of the upstream terrain that is not included in the computational domain such as the terrain upstream of the inlet plane (Wieringa, 1992).

These wall functions replace the actual roughness obstacles but they should have the same overall effect on the flow as these obstacles. This roughness is expressed in terms of the aerodynamic roughness length y_o or less in terms of the equivalent sand-grain roughness height for the ABL,$k_{s,ABL}$, which is typically quite high(large scale roughness, in the range 0.03-2m , $k_{s,ABL}$ in the range 0.9-60m). Note that in CFD simulations, often the upstream part of the domain and the terrain outside the domain upstream of the inlet plane are

assumed to be of the same roughness, implying that it is not the intention to simulate the development of an internal boundary layer (IBL) starting from the inlet plane. In the centre of the computational domain, where the actual obstacles are modeled explicitly, additional roughness modeling is limited to the surfaces of the obstacles themselves (walls and roofs) and the surfaces between these obstacles (streets, grass plains). This is often also done with wall functions. The roughness of these surfaces is most often expressed in terms of the roughness height k_s that is typically quite small (small scale roughness, k_s in the range 0-0.01m).

2.3.6 Validation and verification

For the evaluation of CFD codes it is necessary that all the errors and uncertainties that cause the results of a simulation to deviate from the true or exact values are identified. The most general discrimination divides them into two broad categories

- Errors and uncertainties in modeling the physics
- Numerical errors and uncertainties

Verification and validation (V&V) are the primary means to assess accuracy and reliability in computational simulation. The fundamental strategy of validation is to assess how accurately the computational results compare with the experimental data, with quantified error and uncertainty estimates for both. It is emphasized that there is no fixed level of credibility or accuracy that is applicable to all CFD simulations.

Briefly, verification is the assessment of the accuracy of the solution to a computational model by comparison with known solutions. Validation is the assessment of the accuracy of a computational simulation by comparison with experimental data.

The typical validation procedure in CFD, as well as other fields, involves graphical comparison of computational results and experimental data. If the computational results generally agree with the experimental data, the computational results are declared validated. Comparison of computational results and experimental data on a graph (Oberkampf and Trucano, 2002).

2.4 Tropical climate and environment

The actual levels of the ambient air temperature, solar radiation and wind can be modified by the design details of the outdoor spaces (Givoni et al., 2003). Air movement is considered one of the factors with special significance that is influencing thermal comfort, however; there are limited studies covering the relationship between urban geometry and thermal comfort in hot humid cities (Al-Sallal and Al-Rais, 2012).

It is quite important, therefore; to study the effect of natural ventilation on outdoor thermal comfort and link it to different urban geometries. Moreover, and due to its major impact on building energy, ventilation plays a vital role in designing building systems and it affects directly the amount of building energy consumption. Thus ventilation, and in particular, natural ventilation is one of the means that will help significantly in reducing buildings energy consumption on both architectural and urban scales (Al-Sallal and Al-Rais, 2012).

A study indicated that the geometry of open spaces played a decisive role in thermal distribution. It could be improved by the correct orientation of buildings for shading, while ensuring adequate sky view factor(svf) in order to moderate the harshness of the climate (Bourbia and Awbi, 2004).

There are several factors affecting outdoor thermal environment such as solar radiation, ground surface temperature, air movements around buildings and humidity. amount of both incoming and outgoing radiation and affects also wind speeds (Fahmy and Sharples, 2009).

There are study about the influence of urban geometry on outdoor thermal comfort taking the street canyons of Fez city, morocco as case studies with real site measurements for a period over 1.5years. The results show a clear relationship between urban geometry and the micro climate at street level. Both deep and shallow street canyons with AR of 9.7 and 0.6 respectively were studies in detail. Deep street canyons (AR=9.7) was 10K cooler than the shallow street canyons (AR=0.6) in the warmest summer days due to shading of buildings during the day. Lower parts of the canyons were in complete shade, consequently, surrounding surfaces remain cool and not warmed up at all. With regards to wind speed, they were lower and more stable in the deep canyon (0.4m/s). Where as the shallow street canyon had an average wind speed of 0.75m/s (Johansson, 2006). Another study indicated that the higher AR the cooler the environment where the SVF becomes smaller and it had a strong influence on air temperature(Bourbia and Boucheriba, 2010).

There are studies focused on the experimental investigation of thermal characteristics of a typical street canyon under hot weather conditions. The temporal and spatial distribution of air and surface temperatures is examined, which emphasis was given on the vertical distribution of air and surface temperatures and the air temperature profile in the centre of canyon. Buoyancy generated mainly from asphalt –street heating resulted in the development of the predominant recirculation inside the street canyon (Niachou et al., 2008a).

There is study of air and surface temperature measurements during hot and cold periods. The results showed that there were less air temperature variations compared with the

surface temperatures due to street geometry and sky view factor (Bourbia and Awbi, 2004). The field measurement consisted of temperature and wind velocity measurements for a number of five consecutive days, during day period. Notwithstanding, more measurements of temperature and wind distribution are needed in order to analyze the thermal and airflow characteristics inside urban canyons (Georgakis and Santamouris, 2006).

A research aims to explore the impact of a complex topography and irregular compact urban forms on wind environment and airflow mechanisms at street level and examine the effect of these phenomena on outdoor thermal environment during the daily cycle under hot and dry climate. Extensive on-site measurements of air temperature, horizontal wind speed and direction were collected simultaneously within the streets and above the roofs. Data analysis showed that the air movements within the streets were closely related to the upwind conditions above the roofs which are dependent on the slope exposure to the wind. Finally, the thermal environment was found strongly influenced by airflow patterns during both summer and winter seasons. This research explores the impact of a complex topography and irregular impact urban structure on the airflow mechanisms at street level and examine effect of these phenomena on thermal environment during the daily cycle (Kitous et al., 2012).

In tropical areas, outdoor environmental stress comes mainly from the intense sunlight and strong winds. There are studies conducted on urban wind patterns (Nakamura and Oke, 1988). However very limited researches have been conducted on urban ventilation phenomena and their effects on thermal environment.

General knowledge and common experience today is that hot parts of the world are becoming hotter. This is attributable to global climate change. Places (particularly urban conurbations) with hot weather and climate, with temperature regularly above 35^{o}C have

already recorded 1^{o}C to 2^{o}C increase in average temperature since 1980. Apart from being the corollary of climate change, temperature increase in rapidly growing urban environment results from changes in ground surface covering , reduction in amount of green areas, and abrupt transformation of the outdoor environment (Wong et al., 2007). The phenomenon of "urban heat island" that accompanies the rapid development of buildings, roads and other infrastructures results in temperature increase (Oke, 1973). The effects of the urban heat island increases with growth in the size of a settlement. Vegetation and the presence of "greenery" in open spaces can change the surface roughness of the landscape, affect air movements and in turn alter local temperatures.

The process of urbanization can increase local temperatures in comparisons to less built up suburban rural areas, creating an urban heat island (Rosenzweig et al., 2005). Urban heat island increases the risk of climatic and biophysical hazards in urban environments. The urban heat island refers to an increase in urban air temperature as compared to surrounding suburban and rural temperatures (Oke, 1982). The maximum difference in temperature between a large city and the surrounding rural area can be as much as 12^{o}C on calm, clear nights when the urban heat island effect is most pronounced. The higher temperature was found at the places near the air conditioners and the heat was accumulated under the urban canopy. Urbanization has primarily affected thermal characteristics of ground surface such as solar reflectivity, thermal evaporation and surface roughness. The concrete and asphalt absorb and store more incoming solar radiation than natural surfaces does. This is to say, the outdoor thermal environment is becoming a serious problem with the rapid development of urbanization and economy (Lu et al., 2007) Mega cities around the world have observed a rise in temperature due to a number of factors, namely, modification of urban surfaces, release of anthropogenic heat to the environment, formation of urban

canyons, and loss of vegetation. Large differences between urban and rural temperature are reported in many cities with core city areas termed as "heat island" (Taha, 1997).

One aspect of development recognized as a major contributor to global environmental degradation is the built environment. The environmental impacts of the built environment include high energy consumption, solid waste generation, rising greenhouse gas emissions, pollution, environmental damage and resource depletion spanning the design construction and operational phases of a project (Masnavi, 2007). Recent studies indicate that buildings are responsible for almost 40 percent of global primary energy use (Huovila, 2007). Tackling the environmental impacts of the built environment, therefore has the potential to bring about important sustainability benefits for the world as a whole. Sustainable design of a particular building, group of buildings or settlement and incorporate principles of low impact design, water conservation, renewable energy and energy efficiency, waste minimization and management, and broader sustainability themes (Bauer et al., 2009).

Malaysia launched its country specific green building assessment tool, known as Green Building Index. It has been developed specifically for Malaysia's tropical climate, environmental and development context, cultural and social needs. As global sustainability agenda gathered pace towards the end of the twentieth century, the Malaysian Government took steps to enshrine the principles of sustainable development into national policy plans. Protection of the environment is given priority in the country's overarching long term policy objective highlighting:' Malaysia must ensure that in the pursuit of economic development and adequate attention will be given to the protection of the environment and ecology to maintain the long term sustainability of the country's development.

Malaysia has a warm and humid climate throughout the year. However, it consists of wet and dry seasons, caused by Southwest and Northeast monsoon. The hot and dry season

usually falls in May and June whereas the wet season with low maximum dry bulb temperature usually falls in November (Sanusi et al., 2013). As a tropical country, Malaysia experiences constantly high temperatures and relative humidity, light and variable wind conditions, long hours of sunshine with heavy rainfall and overcast cloud cover thorough the year. The daily air temperature varies from a low of 24^{o}C up to 38^{o}C while the recorded minimum temperature is usually during night. Malaysia has high humidity while the mean monthly relative humidity ranging from 70% to 90% all over the year varying from place to place and from month to month. Nevertheless, the mean daily humidity can be as low as 42% to as high as 94%. Consequently, these environmental features characterize the tropical climate of Malaysia.

The thermal conditions have not been fully explored in outdoor environments of hot and humid climates. Thermal conditions of outdoor spaces were evaluated based upon the measurement of major climatic parameters (Makaremi et al., 2012).

Lately, environmental issues have gained more societal attention and it has been observed that the building sector contributes considerably to climate change (Malmqvist and Glaumann, 2009).

As the climate experiences abnormal changes, international primary evaluation systems also gradually begun to emphasize overall environmental climate regulation, creation of natural ecological environments, and the development of regional and urban evaluation tools. The warming caused by rapid development of large urban areas has led many countries to become aware of the importance and urgency of greening of urban spaces, leading many countries to actively promote building greening policies.(Chang and Chou, 2010)

The main causes of the urban heat island phenomenon are recognized to be the consequences of increased urbanization and abrupt changes in the outdoor environment. These temperature rises in the urban environment are caused by the changes of the street surface materials and reduction of green areas. The variety of urban grids and buildings generate a wide range of different streets, squats , courts and open spaces that further modify local climate into urban micro climates (Wong et al., 2007).

There are indoor and outdoor modification experiments to study the indirect effect of outdoor air temperature towards indoor air temperature. Relationship between reductions in outdoor and indoor air temperature can results in benefits to the building energy savings in a tropical climate. Importantly, this result confirms the effect of outdoor temperature to indoor air temperature reduction.(Shahidan et al., 2012) Outdoor environment is so much more complex than indoor environment. For example the spatial and temporal microclimatic variations of meteorological variables are often very large. Other reasons for the difficulty include lack of climate control in outdoor spaces (Johansson et al., 2014).

Concluding Summary

Previous work has focused on indoor buoyancy effect. Present research is new and novel. This research studies on buoyancy effect on outdoor airflow surrounding building as airflow is considered to be important factor in outdoor environment. Outcome of this research provides a new insight of design of Green M&E systems in the future in Malaysia.

CHAPTER 3

RESEARCH METHODOLOGY

3.0 Research Methodology

3.1 Overview

Workflow of the study is summarized in sequence as follow:

i. *Permission to gain access to the building for conducting the research*

   Permission is required in order to conduct on-site observation and measurement around the building

ii. *Field measurement around the building*

   Measurements have been carried out at various location and on-site activities have been recorded.

iii. *Conduct CFD modeling via suitable solver to examine the outdoor airflow pattern*

iv. *Quantitative assessment and verification of the CFD simulations*

   Assess and verify CFD simulations by comparison with the measurement result, possibly after enhancement of the CFD simulations

v. *Analysis on the current model and comparison with modified design.*

3.2 Fieldwork measurement

The physical measurement data are averaged to get a more accurate data for CFD boundary condition.

3.2.1 Air temperature

Air temperature near building walls is taken using Alnor Thermo anemometer model 440-A. For each measurement point, the temperature is logged for 3minutes. For the measurement points located near the building wall, it is located 1m away from the building façade while on rooftop, it is located 1m away from the roof. (Perini et al., 2011).

3.2.2 Air velocity

For air velocity, a hot wire meter, which is directionally sensitive, had been used during the measurement. The use of this equipment demands for knowledge of primary flow direction. During the fieldwork measurement, the air velocity is measured in three orthogonal directions. At each measurement point, the air speed shall be recorded for minimum 3 minutes with the sampling interval of every 2-4 seconds. For the measurement point located near the building wall, it is located 1m away from the building façade while on rooftop, it is located 1m away from the roof (Perini et al., 2011).

3.2.3 Surface temperature

Wall and ground surface temperature were measured using Campbell Scientific 110PV Surface Temperature Probe. Wall temperatures were measured at the center of the main exterior surfaces of the building. Wall and ground surface temperature is taken hourly

which logged for 5 minutes for each measurement. All surface temperature were monitored and later averaged for a mean value (Rajapaksha et al., 2003). The measurement point for wall is identified for each exterior wall of subject building. Ground surface measurement point is identified at 5m and 10m away from the building.

3.2.4 Ambient site climate

Ambient climate parameters including air temperature and air velocity are taken. It is taken at 2 vertical levels, which are 1.5m and 3m from ground. The measurement point is at an open area.

3.2.5 Building's dimension

Building's dimension is get from the as-built drawing, which is needed in CFD modeling.

3.2.6 Fieldwork summary

From the hourly data collected from fieldwork, it is averaged to be daily data which will be further averaged when input into CFD simulation.

3.2.7 Equipment used

Table 3.1 illustrates the list of equipment used during the measurement

Table 3.1: List of equipment.

Instrument	Detail	Accuracy
TSI VelociCalc Air Velocity Meter	Hot wire anemometer is an instrument for turbulent fluid flow. However main disadvantage of this instrument is its sensitivity to flow accounted to cosine law which only senses the normal to wire axis.	Range : 0 – 30 m/s Accuracy : ± 0.015 m/s Resolution : 0.01 m/s Calibration : Yearly Calibration
Campbell Scientific 110PV Surface Temperature Probe	It uses a thermistor to measure surface temperature	Range : -40 – 135 ^{o}C Accuracy : ± 0.2 ^{o}C Resolution : 0.1 ^{o}C Calibration : Yearly Calibration
Alnor Thermo anemometer model 440-A	It measures the temperature, humidity as well as the air velocity	Range : -10 - 60^{o}C Accuracy : ± 0.3 ^{o}C Resolution : 0.1 ^{o}C Calibration : Yearly Calibration

3.3 CFD modeling

3.3.1 Governing Equations

Conservation of Mass

$$\frac{\partial}{\partial x}(\rho U) + \frac{\partial}{\partial y}(\rho V) + \frac{\partial}{\partial z}(\rho W) = 0 \quad (3)$$

In turbulent flow, fluctuation of air velocity occurs. Hence, summation of time-average component and fluctuating component are used in lieu the velocity of each component, which described in equation below.

U = u + u'

V = v + v'

W = w + w'

Substituting the equation above into (3) yields,

$$\frac{\partial}{\partial x}(\rho u) + \frac{\partial}{\partial y}(\rho v) + \frac{\partial}{\partial z}(\rho w) = 0 \quad (4)$$

The direct implications of the mass conservations in CFD is the continuity of flow, which gives an idea the increase in velocity in any component, will cause the reduction in velocity in adjacent component, since the mass flow in to any control volume must be conserved.

Conservation of Momentum

For X-direction (U-momentum)

$$\frac{\partial}{\partial x}(\rho UU) + \frac{\partial}{\partial y}(\rho UV) + \frac{\partial}{\partial z}(\rho UW) = -\frac{\partial P}{\partial x} + \mu\nabla^2 U \quad (5)$$

For Y-direction (V-momentum)

$$\frac{\partial}{\partial x}(\rho UV) + \frac{\partial}{\partial y}(\rho VV) + \frac{\partial}{\partial z}(\rho VW) = -\frac{\partial P}{y} + \mu\nabla^2 V + \rho\beta g(T - T_{\infty}) - \rho g \quad (6)$$

For Z-direction (W-momentum)

$$\frac{\partial}{\partial x}(\rho UW) + \frac{\partial}{\partial x}(\rho VW) + \frac{\partial}{\partial x}(\rho WW) = -\frac{\partial P}{\partial z} + \mu V^2 W \quad (7)$$

P = static pressure

μ = fluid dynamic viscosity

Conservation of thermal energy

$$\frac{\partial}{\partial x}\left(\rho U\tilde{T}\right) + \frac{\partial}{\partial y}\left(\rho V\tilde{T}\right) + \frac{\partial}{\partial z}\left(\rho W\tilde{T}\right) = \frac{\partial}{\partial x}\left(\frac{\mu}{\sigma}\frac{\partial T}{\partial x}\right) + \frac{\partial}{\partial y}\left(\frac{\mu}{\sigma}\frac{\partial T}{\partial y}\right) + \frac{\partial}{\partial z}\left(\frac{\mu}{\sigma}\frac{\partial T}{\partial z}\right) \quad (8)$$

Where diffusion coefficient, $r = \frac{\mu}{\sigma}$

And $\sigma = \frac{\mu C_P}{\lambda}$ is the Prandtl number of fluid.

3.3.2 Modeling Approach

The objective of current study is to capture an insight on buoyancy effect to air distribution around the building. The flow pattern and the overall picture of possible air flow have to be estimated. The simulations done illustrated a steady state condition.

CFD software ANSYS is chosen in this study because ANSYS Workbench platform directly couples with CAD software and automatically extracts and meshes fluid volumes. From CAD import to geometry meshing, the flexible tools allow to automatically create meshes or hand-craft them. ANSYS meshing can extract fluid volume from a CAD assembly and automatically create tetrahedral or hexahedral meshes with inflation layers. The simulation was performed by using ANSYS Workbench 12.0. It equips with design modeler, meshing, Fluent and CFD Post, which allow users to perform the simulation in a single interface. Details of the software are available at ANSYS (ANSYS, 2009b).

3.3.3 CFD modeling of building

After building the physical model with SolidWork CAD, the model is then imported into ANSYS Design modeler, which the outdoor air space from the physical model is frozen, and the airspace is filled as fluid domain. Then the physical model is subtracted from the entire domain, leaving the fluid domain alone. Subsequently the fluid domain is meshed and ready for the setting of CFD simulation of Fluent.

Throughout this study, the windows are represented as wall. The surrounding environment had been modeled in the simplest dimension. One must use judgment in each case to ensure that the modeled airflow is as realistic as possible within the time and computer resources available.

3.3.4 Computational domain

The computational domain should be large enough to avoid artificial acceleration of the flow. Its size can be based on the height of the building as well on the blockage ratio. In order to avoid inaccuracy in simulation result caused by domain size, the building was located at the middle of the domain, lateral and top boundary were set at 5H away from the blockage, inlet boundary was set as 5H and outlet boundary was 10H away from blockage, where H is the height of the building (Tominaga et al., 2008). The domain roof must be tall enough that no signature of turbulence from lower layers affects airflow at roof layers.

3.3.5 Meshing

The first step in CFD simulation is to discretize the computational domain, which is also called mesh generation. Mesh quality is critical to CFD computations. First, the generated mesh should preserve the correct geometry forms of various objects in the simulation with little amount of manual interaction. Second, the generated mesh should be able to facilitate the computational model to capture the characteristics of the flow fields and the heat and mass transfer process bounded by the geometric set up o the model. For example the regions near the boundary of objects have high gradient of velocity and shear stress reaches the maximum (Zhang et al., 2010).

Enough grids must be initiated in the domain to accurately simulate the interaction of the gas flow with the domain features. However, one also wants to minimize the number of cells in the domain in order to shorten the length of time the computer has to run to solve the problem. This can be most easily accomplished by placing a high concentration of cells around the subject obstacles. The domain edges can have a lower concentration of cells because there is little change in the flow field gradient away from obstacles.

Grid independency test is done to ensure the CFD result is not affected by the meshing. Different sets of model with varies grid number is simulated and the result are compared among each other. When the results showed similar value, it can be said that the model is grid independent.

3.3.6 Boundary Condition

The domain walls must be initialized as proper boundaries. The domain floor will be initialized as a "wall" to simulate the impermeable ground surface. The domain roof and sides can be initialized as "equal pressure" barriers, to ensure that air can flow evenly in or out of the domain depending on the wind field, or for the two walls at the appropriate sides, as "inlets" for air flowing into the domain at the defined wind speed and direction.

The wind entering into the simulated region is not even. According to references and data results, the leading wind direction is influenced by the friction of different kinds of underlying surface. And when it enters into the simulated region, it should distribute under the rule of boundary layer, which is gradient wind. The detailed wind speed is computed,

$$\frac{U}{U_g} = \left(\frac{Z}{Z_g}\right)^{0.28} \tag{9}$$

where U_g is wind speed at the base plane, Z_g is the height above the ground at the base plane. The ground surface temperature is set according to average surface temperature from the physical measurement.

3.3.7 CFD setting

Each cell is initialized with a horizontal wind direction and speed, an initial atmospheric pressure and temperature and local turbulent intensity. No vertical velocity is provided in the initialization but is allowed to develop as the model evolves just as some of the cells close to walls will evolve lower horizontal velocities.

For the near wall treatment, standard wall functions are used. Standard wall functions give reasonable accuracy for a majority of high-Reynolds number, wall bounded flows. The standard wall functions are made of the momentum equation which leads to the law of the wall for the temperature and depends on the y*. A non dimensional wall distance of y+ > 30 is achieved at all computational nodes adjacent to wall surfaces as recommended. The sand-grain roughness k_s is employed to describe the surface roughness. The standard wall function in Fluent between k_s and roughness length y_o has been established as

$$K_s = 9.793\, y_o / C_s \qquad (10)$$

C_s is roughness constant (Blocken et al., 2008). Value of k_s cannot larger than y_p which is the distance between the centroid of the wall-adjacent cell and the wall.

3.4 Verification of CFD

Confirmation on the predicted result should be carried out to ensure the discretization method, grid resolution is correct on performing the task. Verification is a process to ensure the physical or mathematical model could represents the conceptual description and the solutions of the model accurately.

The comparison between the simulation and on-site measurement should start by comparing the airflow pattern qualitatively. Upon the qualitative comparison, it should

follow by assessment of first order parameter such as air velocity. Despite of describing the results from comparison qualitatively (such as excellent, poor, fairly, etc), it should come along with quantitative comparison, and provide the judgment by referring to other literatures available. Moreover, if the result obtained from the simulation have a lesser accuracy, it could be considered acceptable as long as the predicted trends are consistent.

CHAPTER 4

CASE STUDY OF GREEN BUILDING

4.0 Case study of green building

4.1 Overview of building and surrounding environment

The research subject building is Energy Commission in Malaysia, which is known as Diamond Building due to its architectural design of a diamond shape. This building has a unique architectural feature whereby it can self shade, as shown in Figure 4.1. It is located at Precint 2, Putrajaya Adjacent to Taman Pancarona, a public landscape garden. The Diamond Building was designed and built with the concept of a sustainable building. The diamond shape is found to be the most aerodynamic and effective form to prevent air infiltration through the advantage of tilted façade. The Diamond Building is the first office building in Malaysia to obtain the Green Building Index platinum rating, and the first outside of Singapore to obtain the Green Mark platinum rating. (The Green Mark is Singapore's certification scheme for green buildings.) The Energy Commission's Diamond Building in Putrajaya was named the most energy-efficient building at the Asean Energy Awards (AEA) 2012 held in Phnom Penh, Cambodia. The seven-storey Diamond Building is the first office building in Malaysia to obtain the Green Building Index platinum rating and the first building outside Singapore to obtain the island state's Green Mark platinum rating.

Figure 4.1: Energy Commission, Diamond Building.

Two sides of the building face north and south. While the sun's path is from east to west, it will sometimes tilt to the north or to the south. It is shown in Kuala Lumpur sun path diagram in Figure 4.2. The tilt angle is about 25°, so the building's facade is also tilted at 25° as shown in Figure 4.3. The north and south facades are self-shading. The building will still have the morning sun and afternoon sun in the east and west, but the time of exposure to direct sunlight would also be lessened because of the inclination.

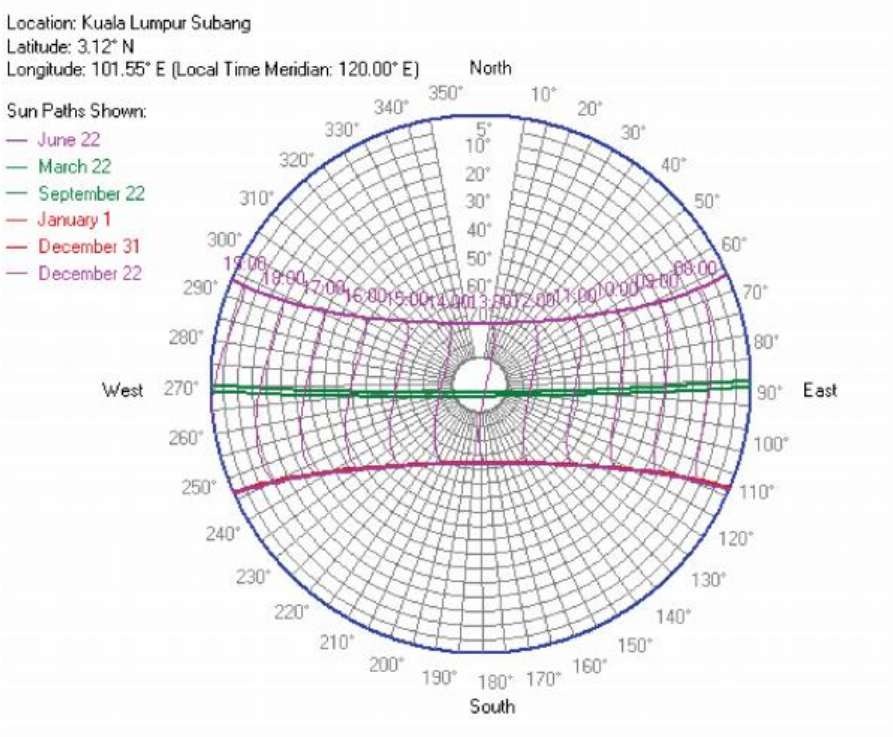

Figure 4.2: Sun path diagram of Kuala Lumpur (Hew & Rap, 2012).

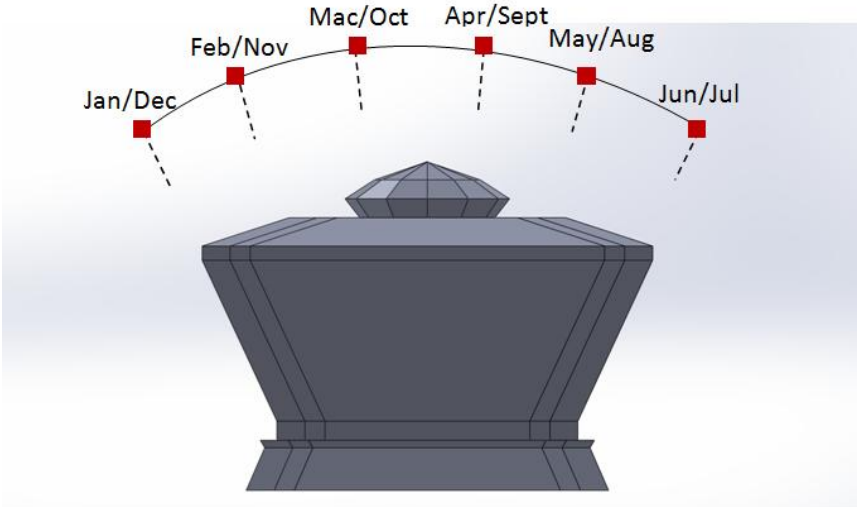

Figure 4.3: Sun path diagram of Diamond Building.

4.2 Physical measurement

The on-site measurement of the building was conducted for two weeks on 1-15 April 2012, the parameters taken such as the surface temperature, ambient air temperature and wind speed. The physical layout and dimension of the building were recorded which will be used in the modeling process. There are total 24 measurement points during physical measurement.

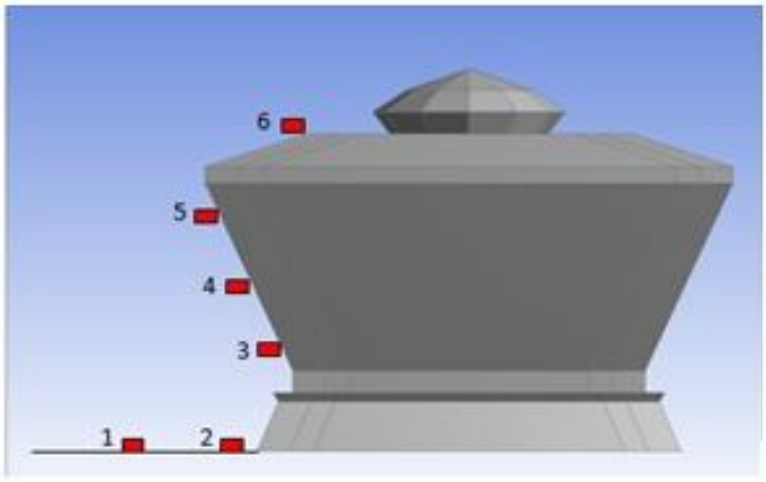

Figure 4.4: Measurement point (side view).

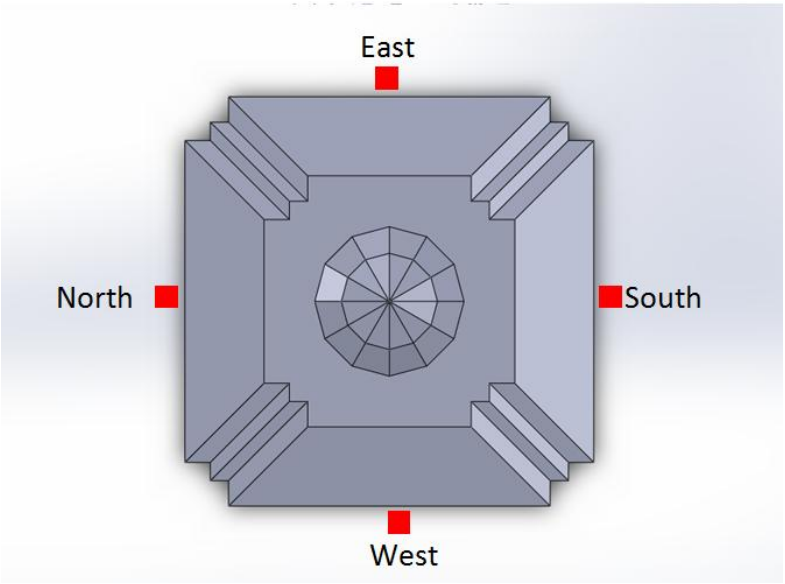

Figure 4.5: Measurement point (top view).

4.3 Air velocity measurement

The measured data are tabulated is plotted in Figure 4.6- 4.8. Y-axis velocity has a repeating airflow pattern while X and Z-axis has random airflow pattern.

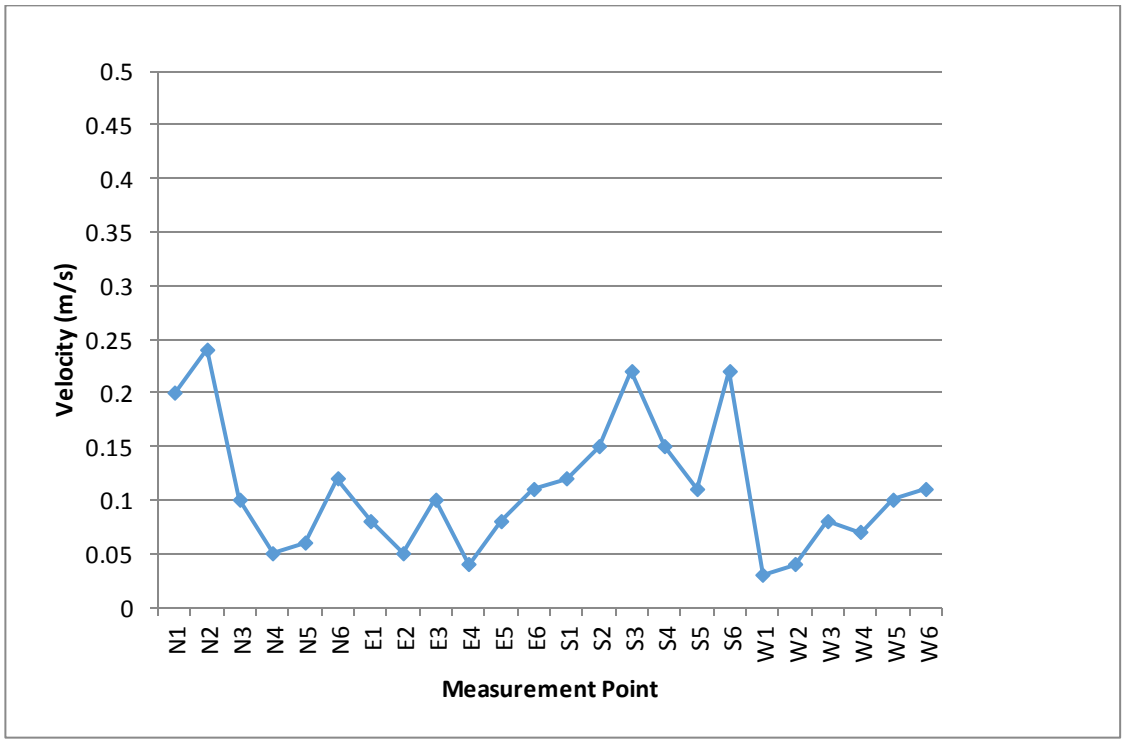

Figure 4.6: X-axis velocity of measured data.

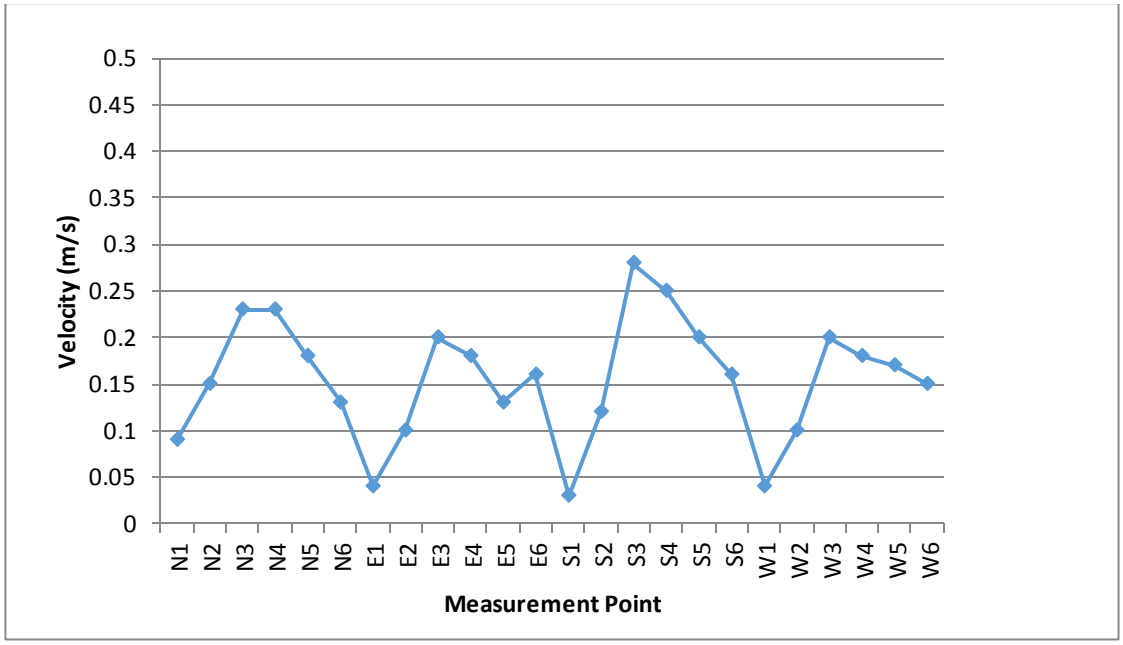

Figure 4.7: Y-axis velocity of measured data.

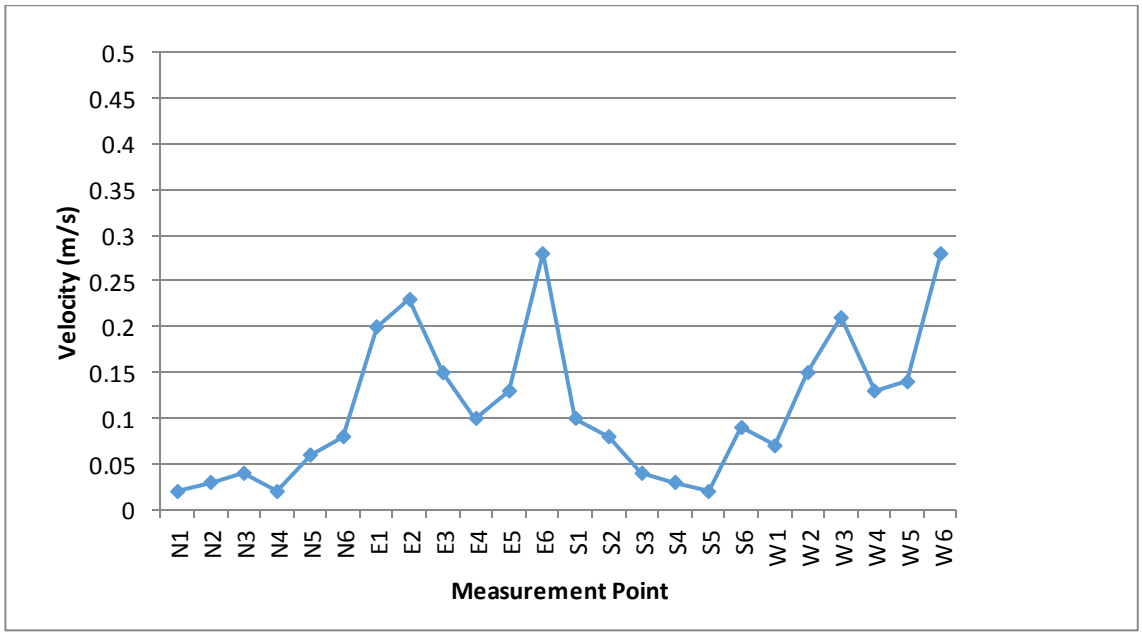

Figure 4.8: Z-axis velocity of measured data.

4.4 CFD modeling

4.4.1 Building modeling

In this research, a few assumptions have been made. The building façade's materials are of uniform thermal character, and there is no heat transfer between the indoor and outdoor of the building. More than 80% of the green building façade is covered by tempered glass, and so the entire building's façade is modeled as the tempered glass. There are some trees around the building, but they are not modeled in the simulation in order to simplify the model. CFD model of building is shown in Figure 4.9.

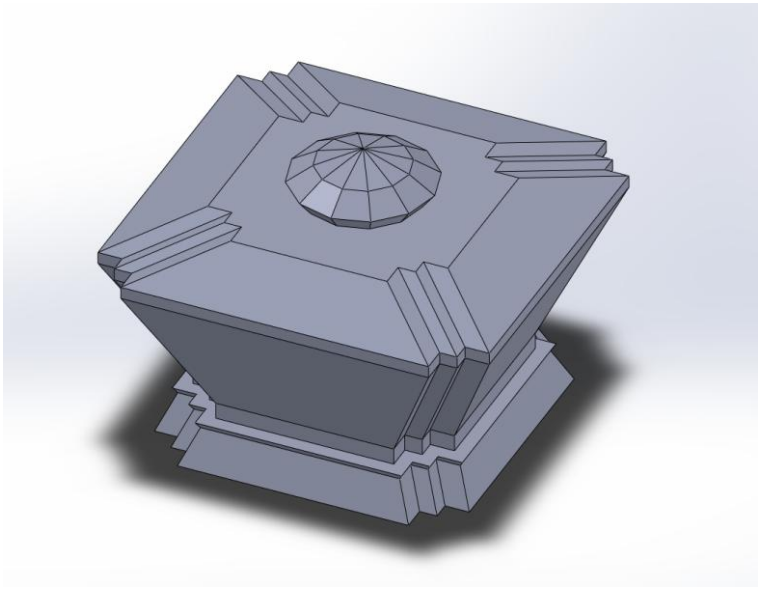

Figure 4.9: Modelling of Diamond Building.

4.4.2 Domain

The domain for the simulation model is set at 11H width, 16H length and 6H height, which is 550 x 800 x 300 m^3 shown in Figures 4.10 and 4.11. The blockage of this model is 0.001% that is much lower than the suggested blockage ratio of 3%

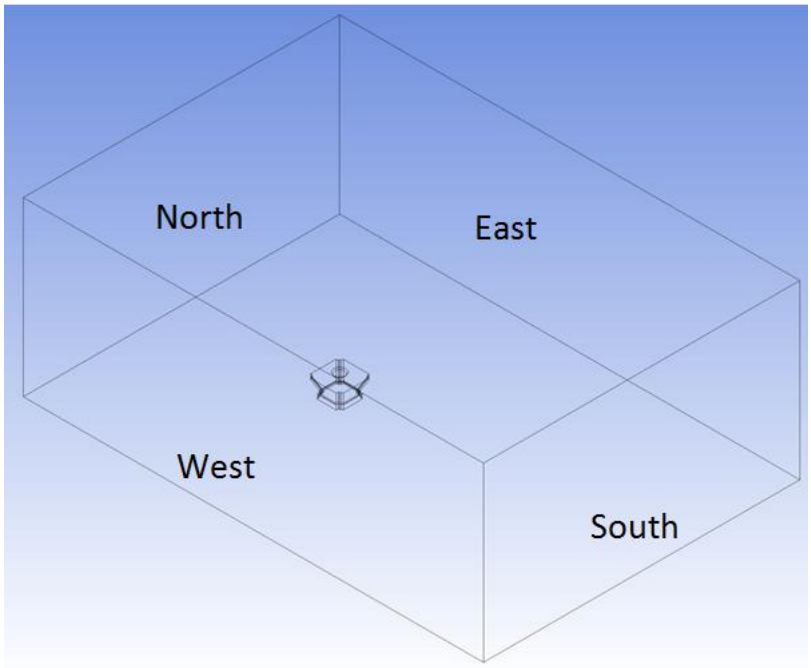

Figure 4.10: Simulation domain (Case 1).

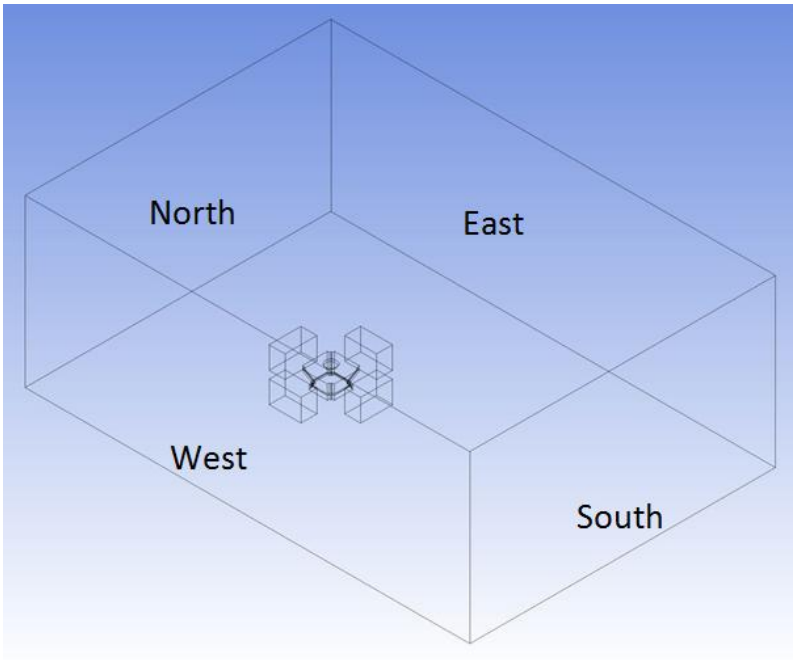

Figure 4.11: Simulation domain (Case 2).

4.4.3 Boundary Condition

Table 4.1: Boundary Condition.

Item	Details
Wind inlet	Applied only for Case 2. Velocity at $3ms^{-1}$ from north wall
Wind outlet	Applied only for Case 2. Pressure outlet was set to zero gauge pressure in south wall
Roof	Set as wall, no-slip condition.
Walls	Set as wall, no-slip condition.
Ground	Set as wall, no-slip condition. It is divided into 2 zones, zone 1 is the shaded ground with 296K, and zone 2 is open ground with 318K

4.4.4 Setting of the simulation

The settings for the simulations are listed in Table 4.2 shown below.

Table 4.2: Simulations settings.

Solver	**Pressure based coupled solver and steady state**
Model	k-Ɛ model, $\sigma_k = 1.0$, $\sigma_e = 1.3$, $C_{1e} = 1.33$ $C_{2e} = 1.92$, $C_\mu = 0.09$ Full buoyancy effects is on to include buoyancy effects on ε. Standard wall treatments.
Solution method	Scheme : SIMPLE Gradient : Least- square cell based Pressure : Standard Momentum : 2^{nd} order upwind Turbulent kinetic energy : 2^{nd} order upwind Turbulent dissipation rate : 2^{nd} order upwind

	Energy : 2^{nd} order upwind
Solution Control	Under relaxation factor Pressure : 0.3 Density : 1 Body forces :1 Momentum :0.7 Turbulent kinetic energy: 0.8 Turbulent dissipation rate : 0.8 Turbulent viscosity : 0.5 Energy: 1
Convergence criterion	Continuity, x,y,z-velocity, k, epsilon : 5×10^{-4} Energy : 1×10^{-7}

4.5 Mesh independence

For grid independent study, five different numbers of meshing element were examined, in tetrahedral meshing. The number of elements is corresponding to 100, 80, 60, 40 and 20 in fine relevance center at Workbench meshing setting for Mesh I, II, III, IV and V respectively. The detail of the mesh independence test is shown in Table 4.3. Velocity profile is visually examined. Similar pattern are found in Mesh II, III, IV and V. Air velocity is examined and the results from different mesh elements are plotted in graphs as shown in Figure 4.12. The solution approaches a constant value as the number of mesh increases and Mesh IV and V have same value. Mesh III is adopted as it is adequate to perform the simulation accurately.

Table 4.3: Results for Mesh Independency test.

Mesh No.	Number of elements	Representative mesh size, h (m)	Ratio, h(n)/h(n+1)
I	905164	4.026	
II	1404392	3.200	1.15
III	2013944	2.830	1.13
IV	2487546	2.644	1.07
V	3310963	2.404	1.10

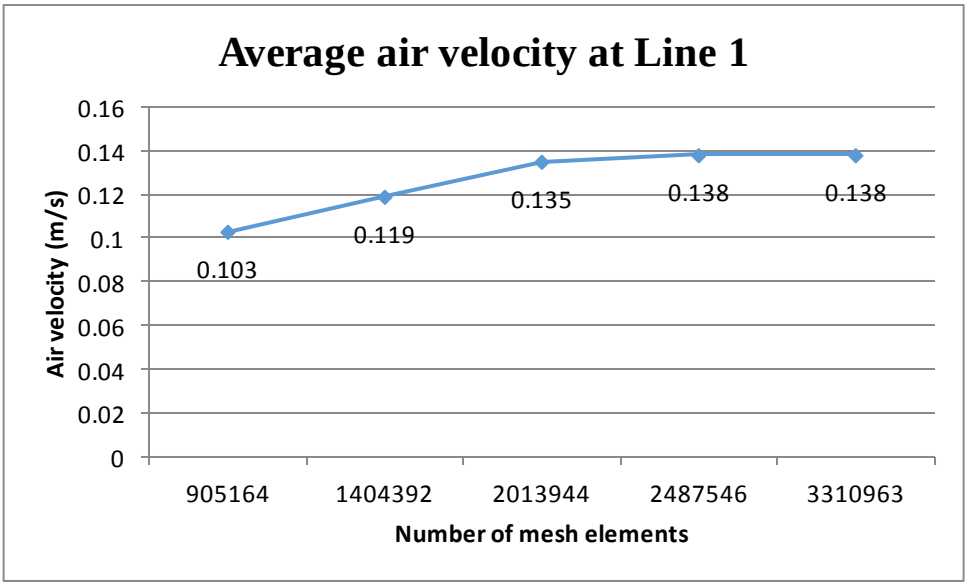

Figure 4.12: Results for mesh independency test.

4.6 Verification of model

Figures 4.13 to 4-15 show a close qualitative agreement between the fieldwork data collection and the CFD simulation result. It is noticeable that both results have the similar trend.

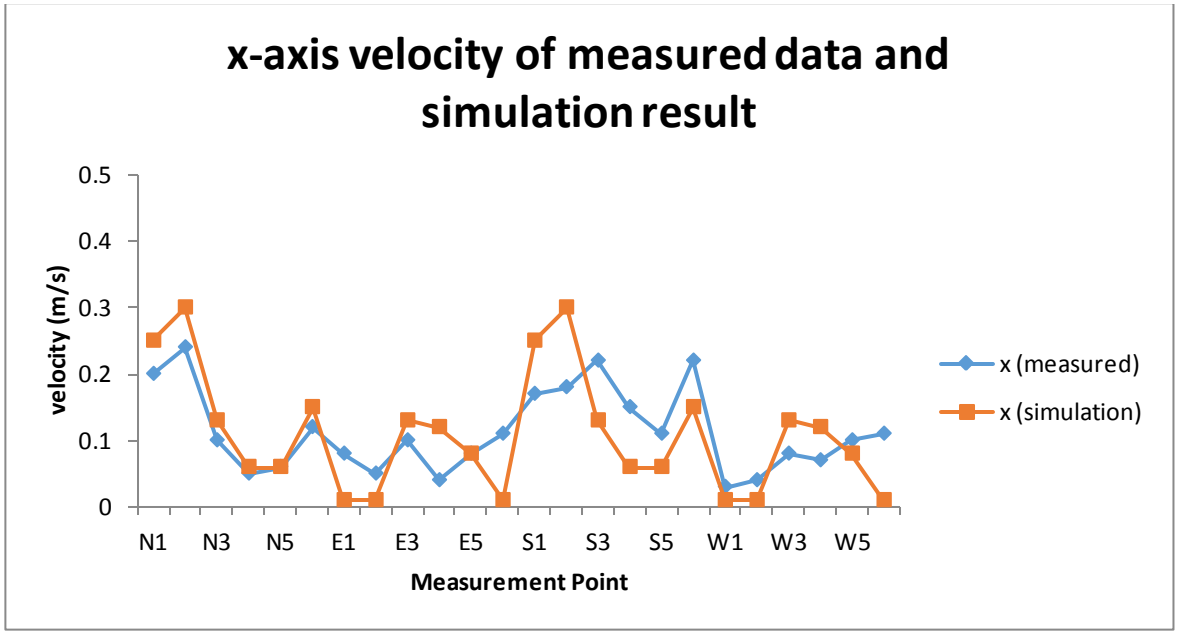

Figure 4.13: X-axis velocity of measured data and simulation result.

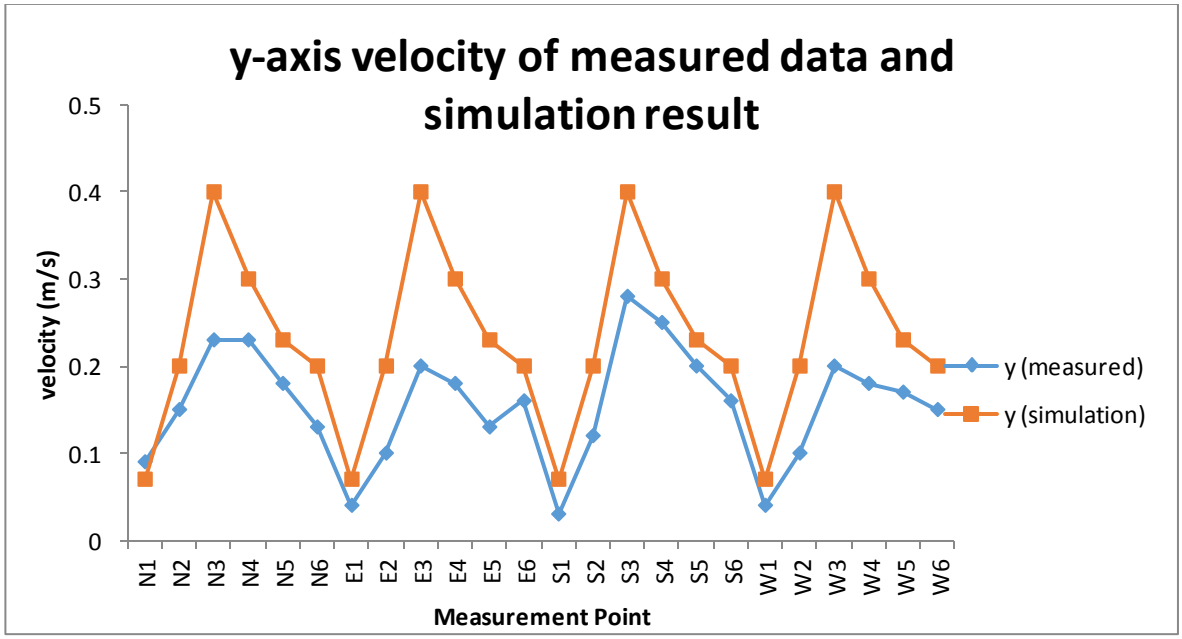

Figure 4.14: Y-axis velocity of measured data and simulation result.

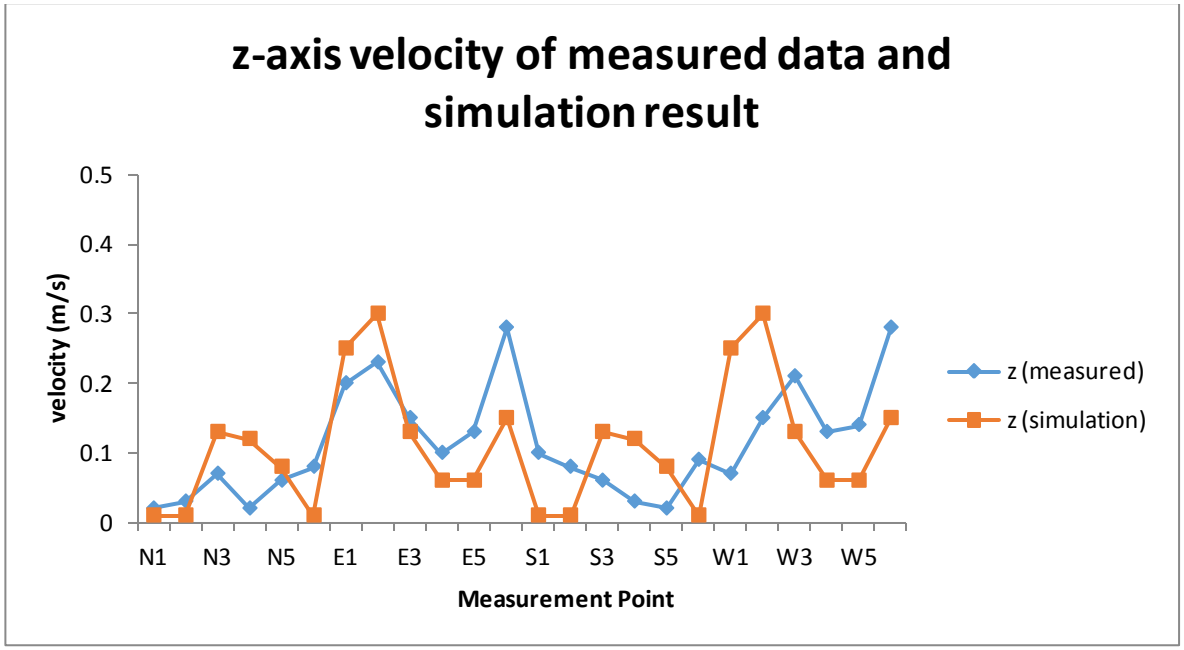

Figure 4.15: Z-axis velocity of measured data and simulation result.

Table 4.4 shows the bias uncertainty analysis of the simulation results with fieldwork measurement. Maximum value between physical measurement and simulation has less than 20% of error, which is acceptable. For minimum value, the error of percentage is up to 50% which the value of bias is only 0.02ms^{-1}. The deviation shown is probably due to the assumptions made in the present study. In evaluation on whether the simulation result is acceptable compared to field measurement, the error reported between 15-20% can be considered as good agreement (Memarzadeh & Jiang, 2010).

Table 4.4: Bias uncertainty analysis.

Axis	$Min_{Physical}$, ms^{-1}	$Min_{Simulation}$, ms^{-1}	Percentage of error, %	$Max_{Physical}$, ms^{-1}	$Max_{Simulation}$, ms^{-1}	Percentage of error,%
X	0.03	0.01	50.0	0.24	0.30	11.1
Y	0.03	0.07	25.0	0.28	0.40	17.6
Z	0.02	0.02	0.0	0.28	0.25	5.6

4.7 CFD simulation result of Diamond Building

In the discussion, there are two planes had been defined in order to ensure lucidness on the comparisons. Plane YX (side view) cut through vertically at the middle of the model, while plan XZ (top view) is a horizontal plane located 25m from ground level, which is half of the building height.

4.7.1 Case 1

During fieldwork measurement, the surrounding wind flow is approaching 0ms^{-1}. For Case 1, which refers to actual case with non-windy environment, so the air flow surrounding the building was completely induced by the buoyancy effect caused by the surrounding surface temperature difference. Figure 4.16 shows the top view of the model. It is noticed that the air flow was occurred in the zone beneath building's shade. From Figure 4.17, it was clearly seen that the air flow pattern. As the building is self shading, so the air temperature under the shade is cooler than the air temperature outside of the shade. The average temperature difference is 4^{o}C. Cooler building surface draw heat away from surrounding air, which then falls due to increased density. This induced the flow where the cooler air will flow downwards along the façade of the building and the warmer air will flow upwards due to density difference. The air flow induced has air velocity range from 0.17 to 0.69 ms^{-1}. At the upper part of the shade, the flow has the lowest air velocity, which then increasing when then going further down towards the lower concrete wall. The air has highest velocity at the concrete wall. Lower concrete wall has lower surface temperature compared to upper glass façade, which it induced the air flow in this direction. At the top roof, the air flow is flowing upwards, because the air that is adjacent to the roof surface has higher temperature,

this induced it to flow upwards. From the Gr/Re^2, the ratio is 1.98 and is greater than 1 which indicates natural convection dominating.

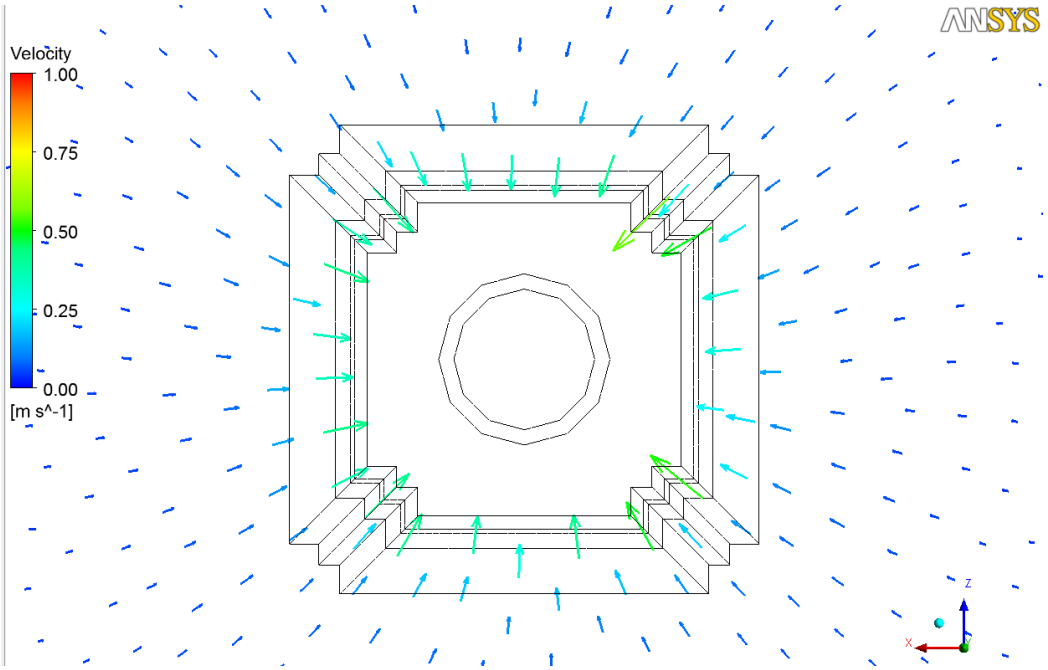

Figure 4.16: Case 1 simulation result (top view).

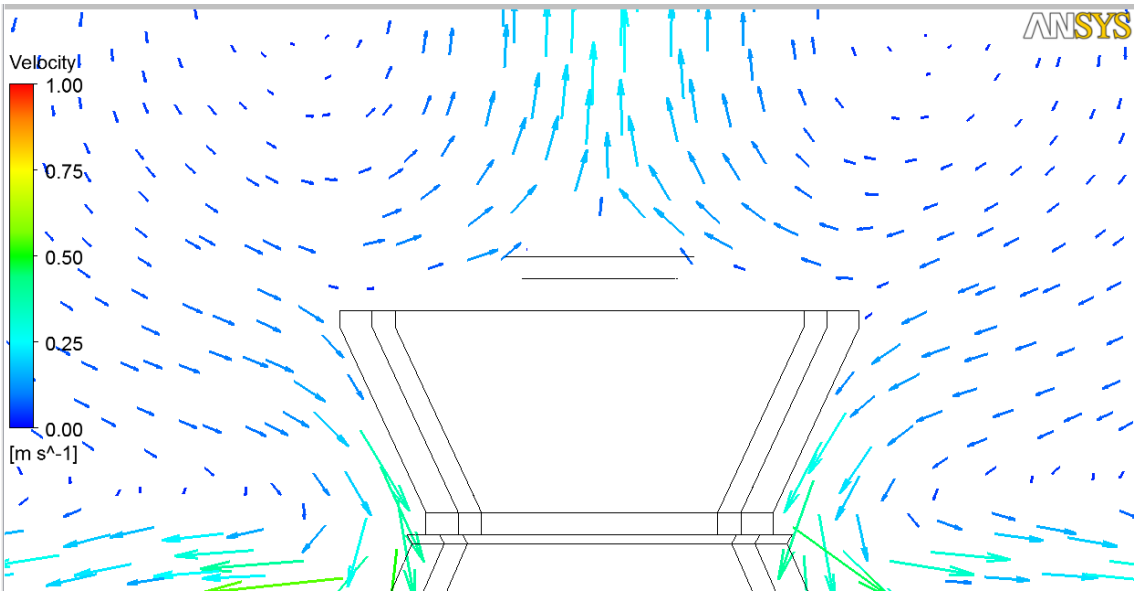

Figure 4.17: Case 1 simulation result (side view).

4.7.2 Case 2

Case 2 has the same condition as Case 1, but there is one more factor added into this case whereby the wind is simulated from the north direction with 3 ms^{-1}. Figure 4.18 shows the top view of the result, the wind had totally contributed to the air flow pattern, which in this case, the buoyancy effect can be totally ignored. It can be seen from the result shown in Figure 4.19, it is turbulent when the incident wind flow in contact with the building and turn to sideway direction. Vortex is formed at the back of the building. It has maximum air velocity of 3.05ms^{-1} at the top of the building. From the Gr/Re^2, the ratio is 0.1 indicating buoyancy effect is insignificant.

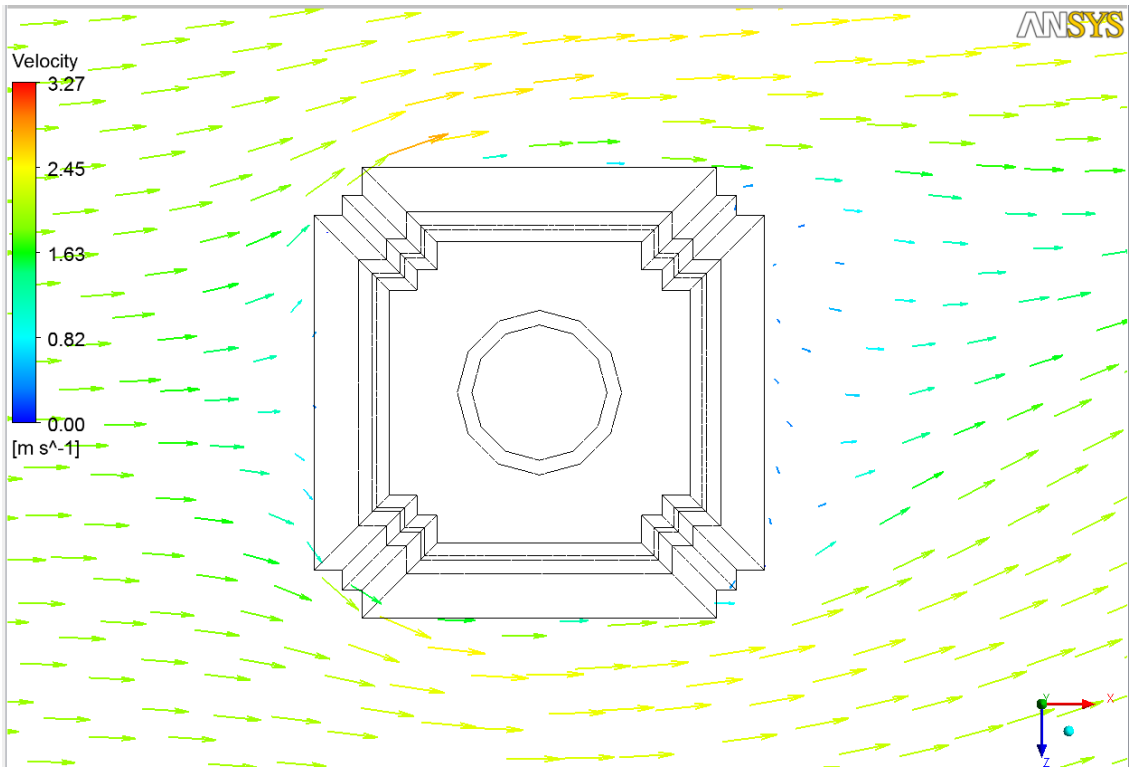

Figure 4.18: Case 2 simulation result (top view).

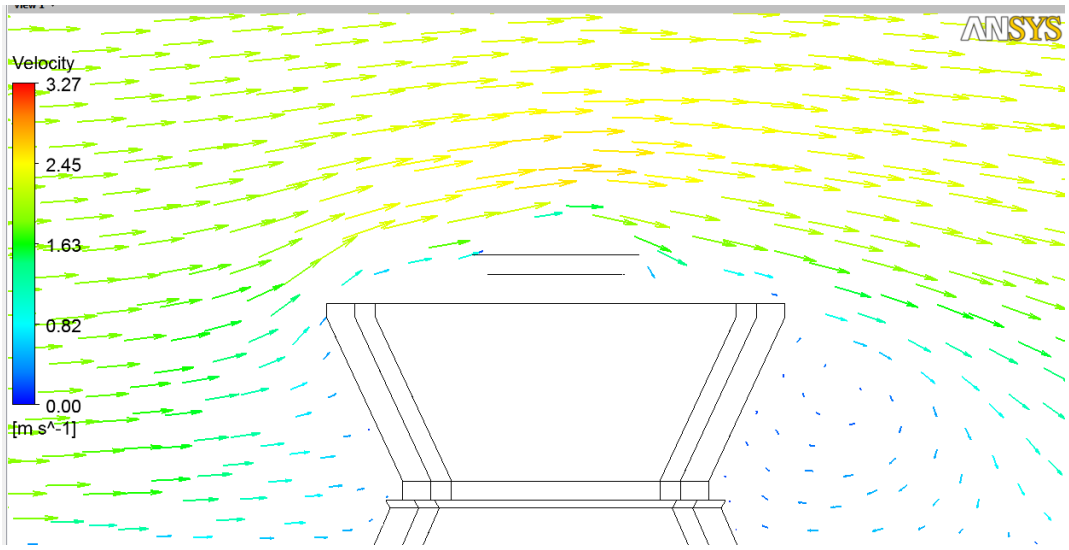

Figure 4.19: Case 2 simulation result (side view).

4.7.3 Case 3

Case 3 simulates future development where the green building is surrounded by other buildings in a slightly dense built area. Four obstacle buildings which are 30m away from the Diamond Building are modeled in this case. As in Case 1, no natural wind is simulated. Figure 4.20 shows the top view of the model. There is air flow under the shade due to buoyancy effect as shown in Figure 4.20. The air flow pattern is similar to Case 1. The flow starts from the top of the shade along the façade to the bottom of the building. The induced air flow velocity is ranged from 0.20 to 0.71 ms^{-1}. From the Gr/Re^2, the ratio is 1.87, greater than 1 which indicates buoyancy effect dominating the airflow.

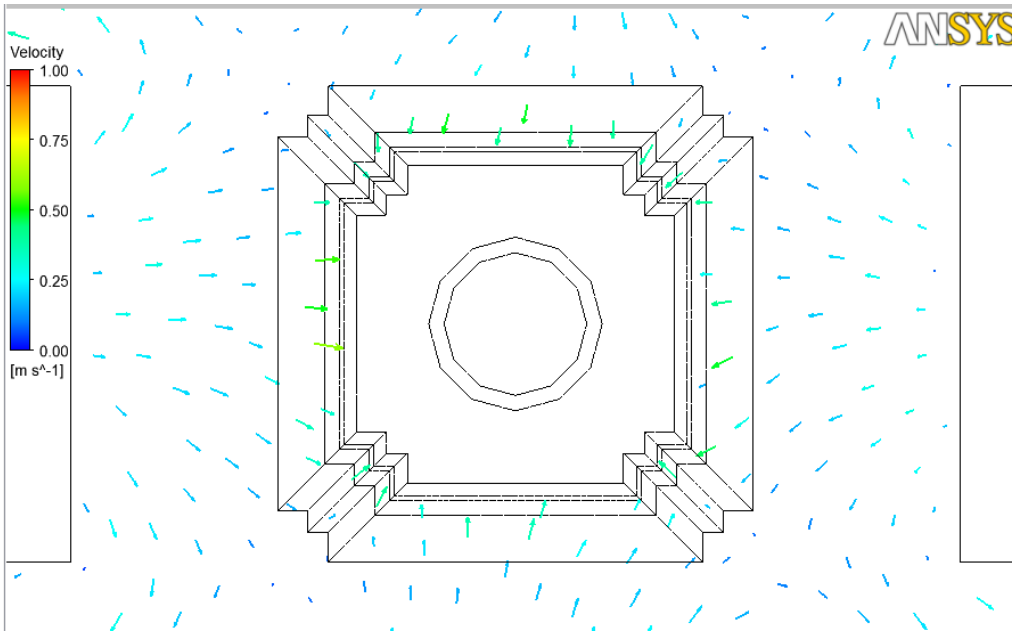

Figure 4.20: Case 3 simulation result (top view).

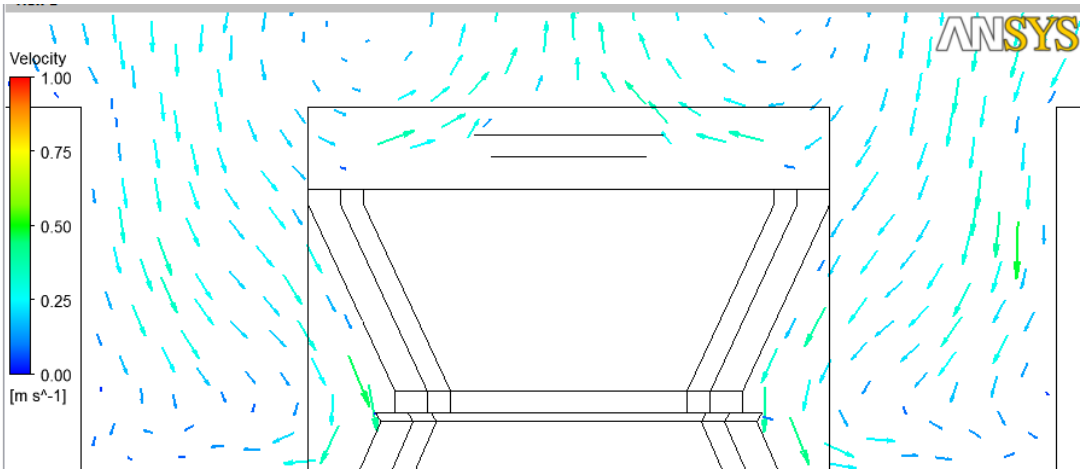

Figure 4.21: Case 3 simulation result (side view).

4.7.4 Case 4

Case 4 has the same model with Case 3 with wind coming from the North direction. As in Figure 4.22, the wind has dominated the air flow direction surrounding the green building. But in the North direction of the green building where the wind is blocked by the adjacent

building, the air flow velocity is relatively low as illustrated in Figure 4.23. The East and West air flows are affected by the wind with maximum velocity of 4.97ms^{-1}. While at the South of the green building, there is a vortex formed because the wind from the top of the green building is directed into the space between the green building and the South building. This happens due to the design of its roof. From the Gr/Re^2, the ratio is 0.04 , much smaller than 1, indicating wind force dominating the airflow.

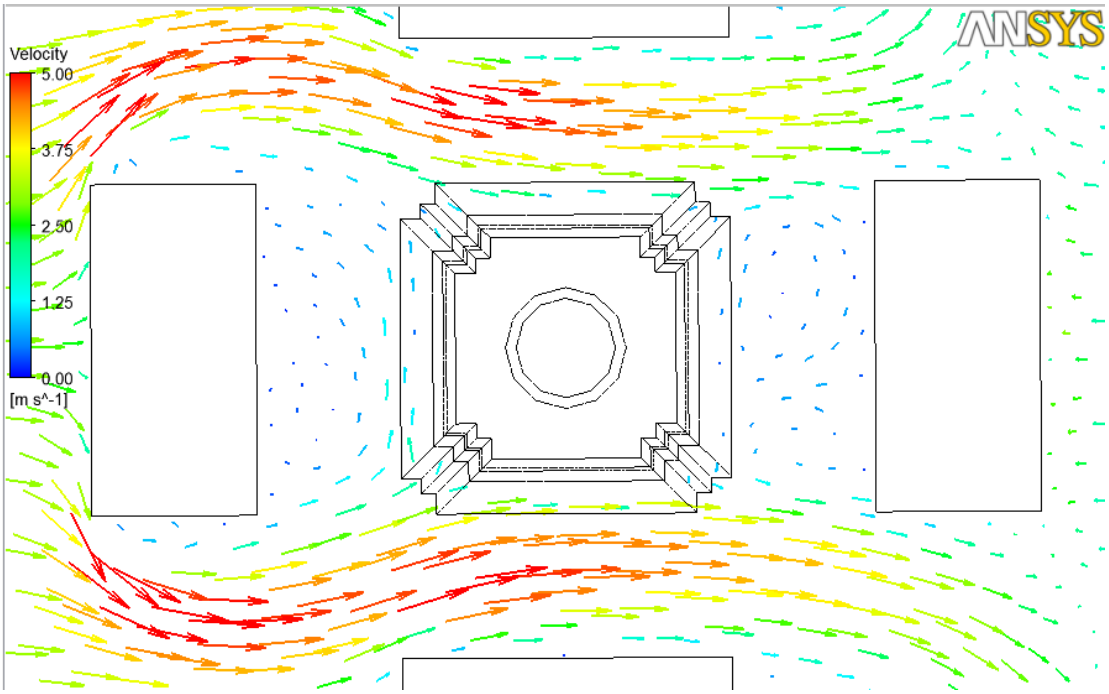

Figure 4.22: Case 4 simulation result (top view).

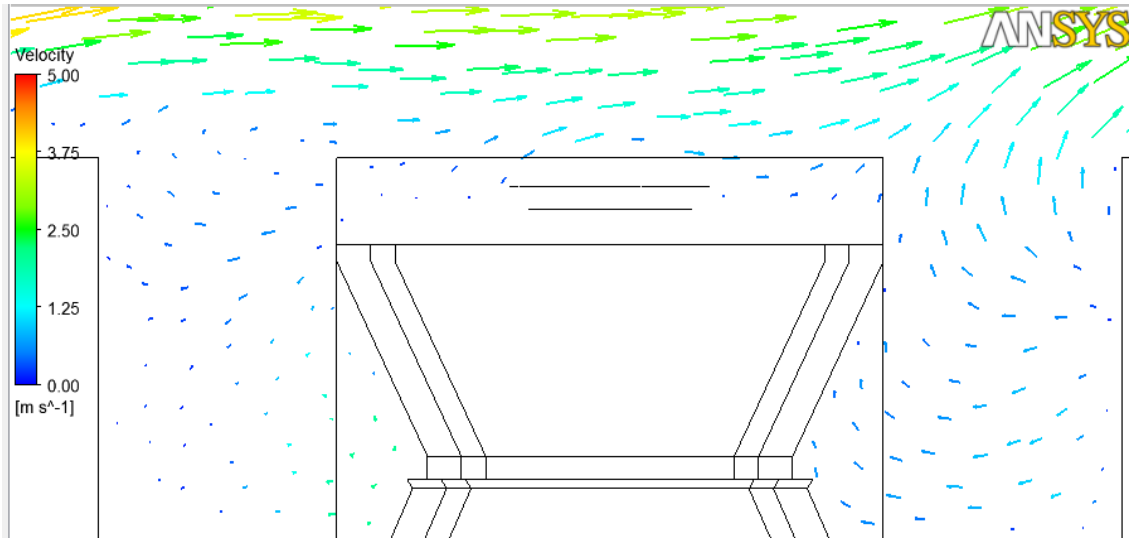

Figure 4.23: Case 4 simulation result (side view).

4.8 Relationship between temperature difference to airflow induced by buoyancy

3 simulations are carried out to study the relationship between outer ground surface temperature and air velocity induced by buoyancy effect. Ground surface is set with 3 different temperatures, which are 318K, the actual condition, 328K and 308K respectively.

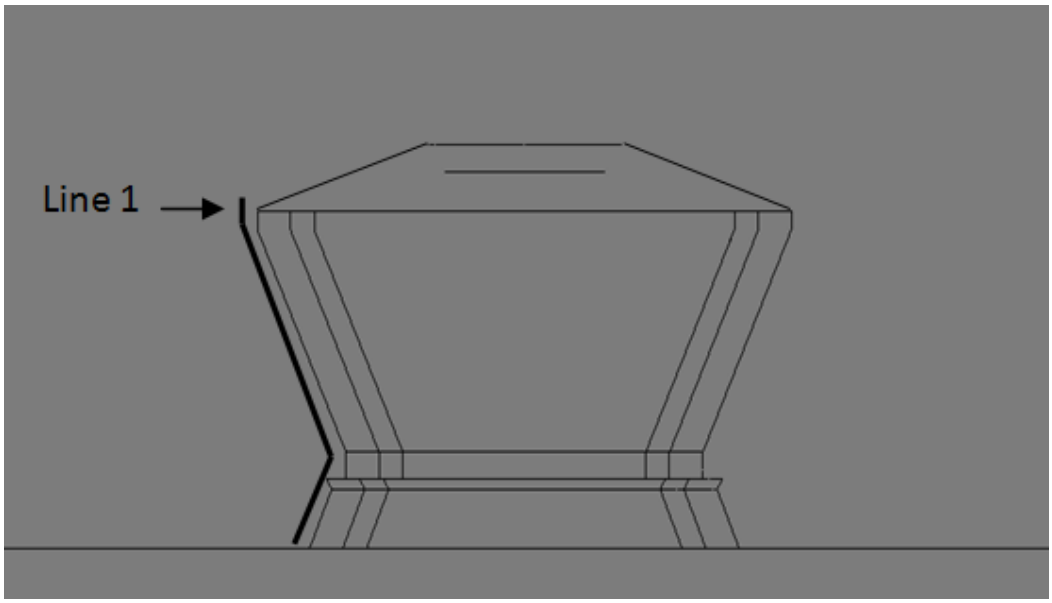

Figure 4.24: Location of Line 1.

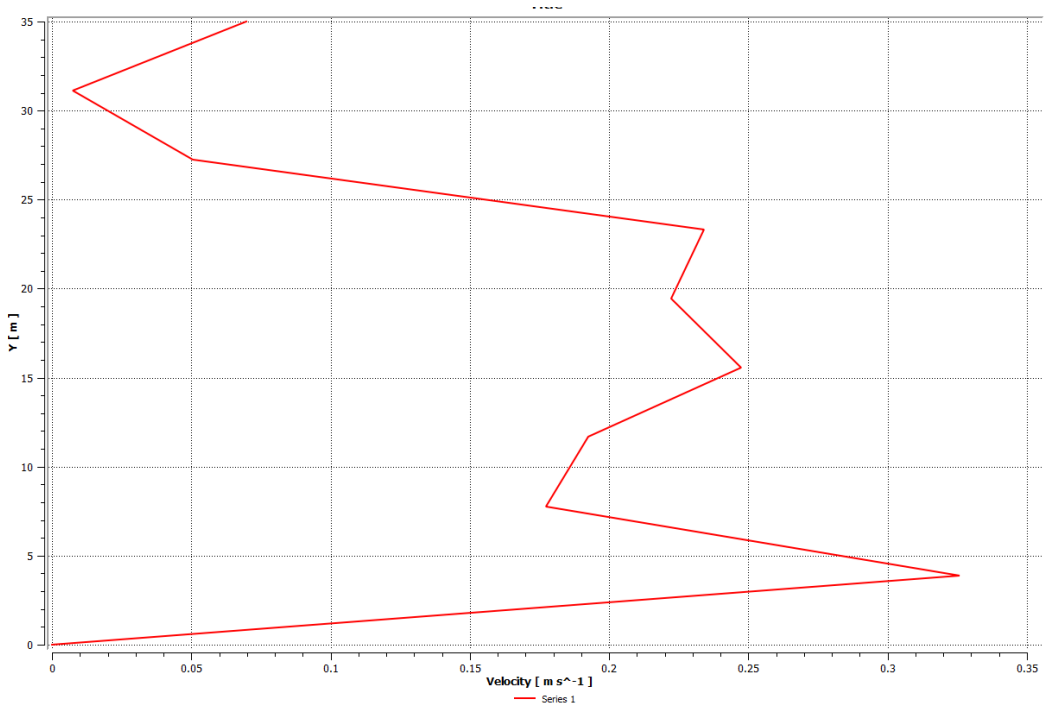

Figure 4.25: Air velocity induced by outer ground surface temperature of 318K.

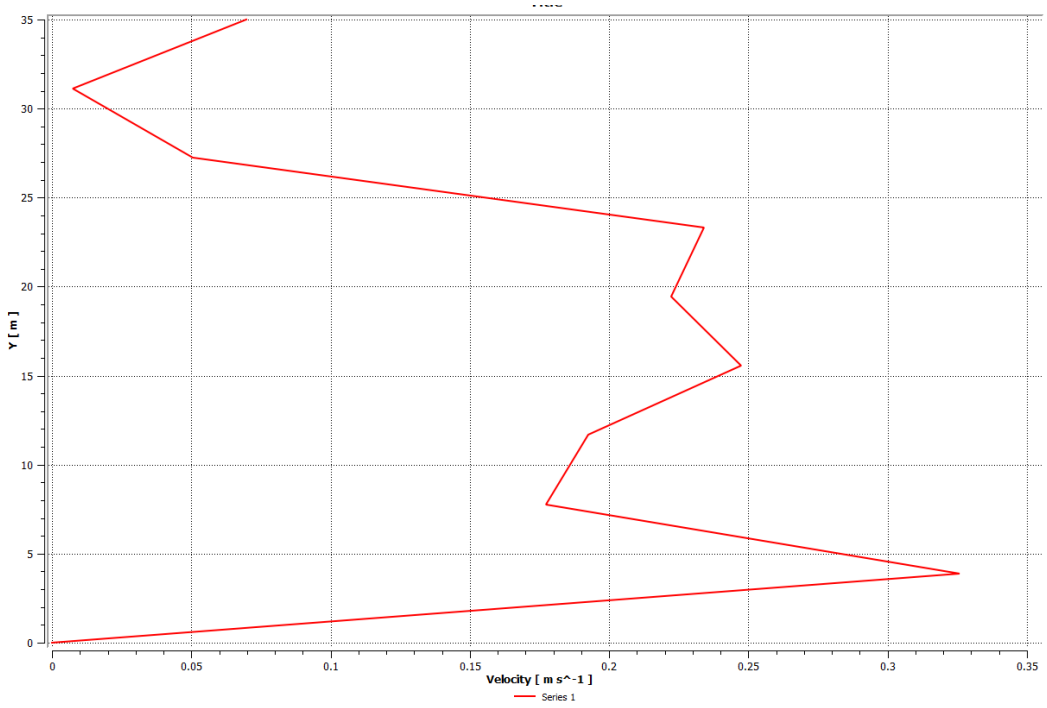

Figure 4.26: Air velocity induced by outer ground surface temperature of 328K.

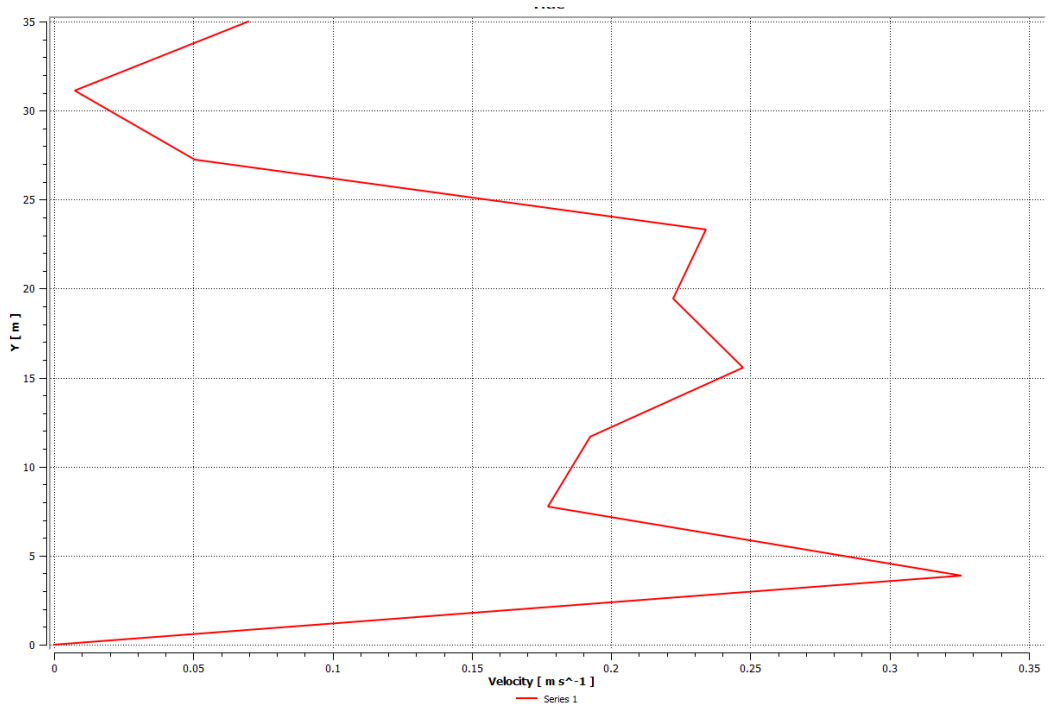

Figure 4.27: Air velocity induced by outer ground surface temperature of 308K.

Figures 4.25 to 4.27 have same air velocity pattern induced regardless of the outer ground surface temperature. This is due to diamond building self-shading feature that regardless the outer ground surface temperature, the ground beneath shaded area of the building maintained the low temperature as in actual condition. Hence, the air velocity profile induced is same with the highest air velocity induced at the bottom of the building.

4.9 Concluding summary

This chapter has demonstrated the effect of buoyancy to airflow surrounding a green building. Two parts has carried out, first part is to study the significance of buoyancy to airflow with and without present of wind. Second part is to study the relationship between temperature differences among surfaces to air velocity induced by buoyancy.

- Buoyancy effect induced the vertical air movement when no wind is present. Whilst, the buoyancy is insignificant when the wind is present as the flow is dominate by the wind force.
- Buoyancy is affected by the temperature difference between surrounding building and ground surface. When the ground surface temperature is greater, the air velocity induced has higher air velocity and vice versa.

CHAPTER 5

CASE STUDY OF CONVENTIONAL BUILDING

5.0 Case study of conventional building

5.1 Overview of building

Sarawak General Hospital Heart Centre (SGHHC) was formerly named as Sarawak International Medical Centre. The hospital was officiated on January 2011. This building is a 8 storey ward tower of Sarawak International Medical Centre (SIMC). Figure 5.1 showed Sarawak General Hospital Heart Centre.

Figure 5.1: Sarawak General Hospital Heart Centre.

5.2 Physical measurement

The on-site measurement of the building was conducted on 3-28 January 2011. The parameters taken such as surface temperature, air temperature and wind speed. The physical layout and dimension of the building were recorded and is used in the modeling process.

There are total 50 measurement points during physical measurement. Figures 5.2 and 5.3 illustrate the location of the measurement points.

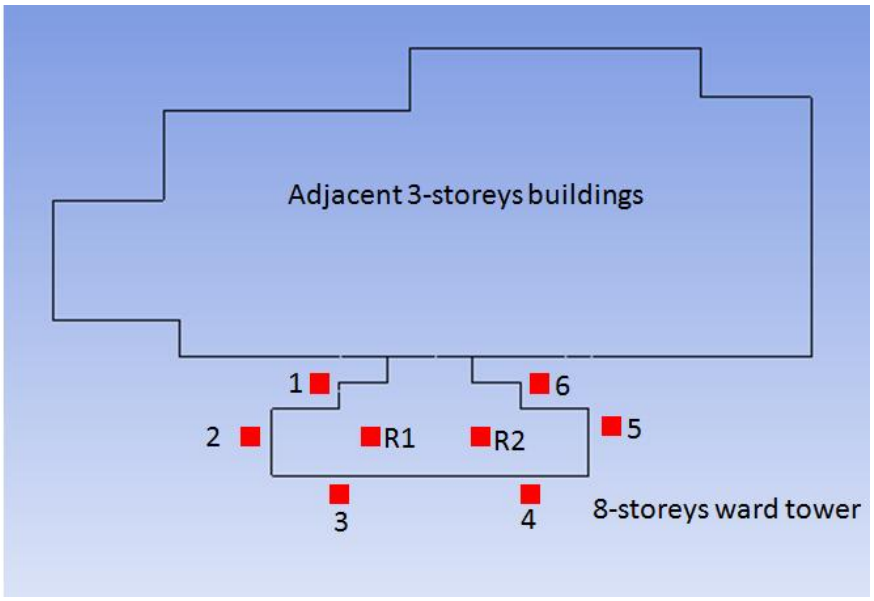

Figure 5.2: Top view of measurement location.

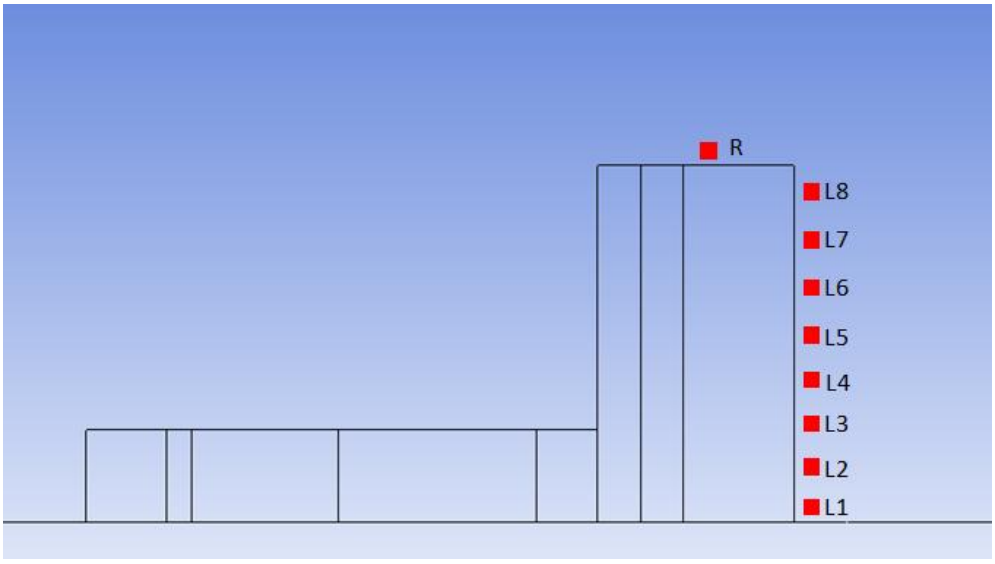

Figure 5.3: Side view of measurement location.

5.3 Air velocity measurement

Air velocity at X, Y and Z-axis are plotted in graph as in Figures 5.4 to 5.6. X and Z-axis velocity are relatively low compared to Y-axis velocity. The maximum air velocity for X, Y and Z-axis are 0.02 ms^{-1}, 0.2 ms^{-1} and 0.03 ms^{-1} respectively.

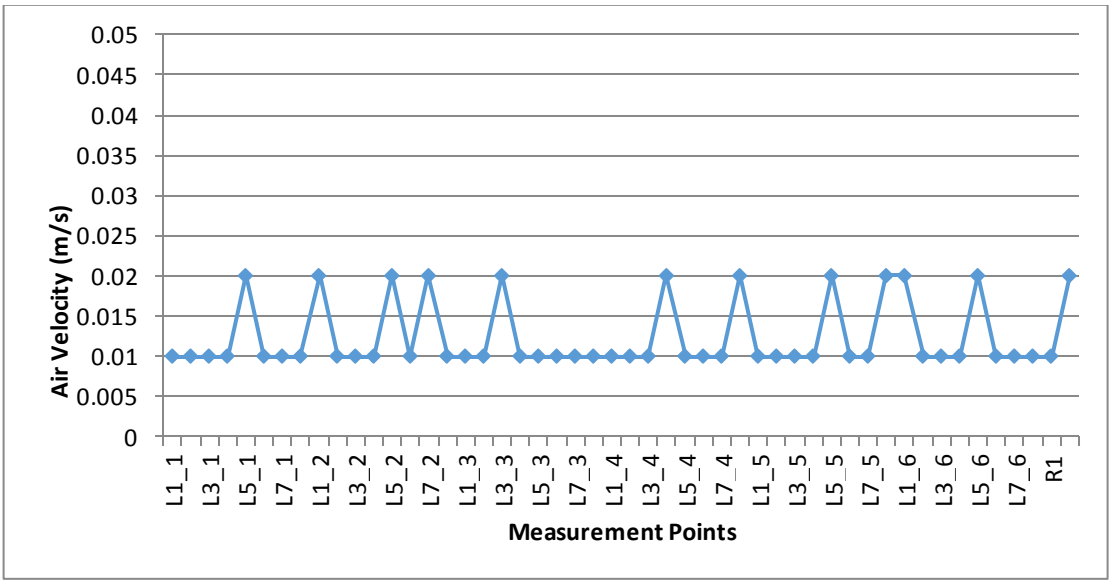

Figure 5.4: X-axis velocity of measured data.

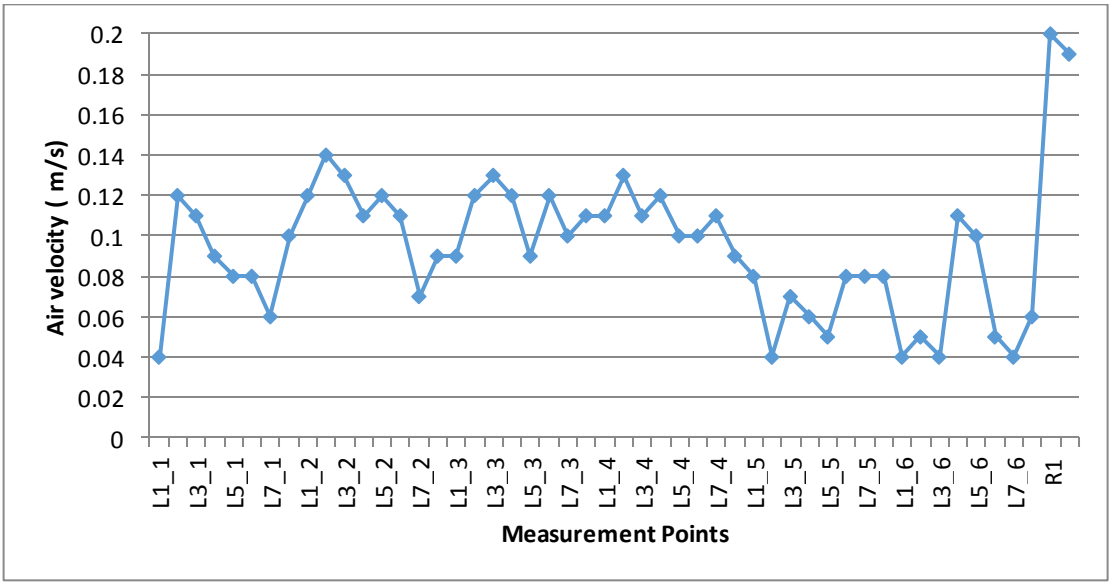

Figure 5.5: Y-axis velocity of measured data.

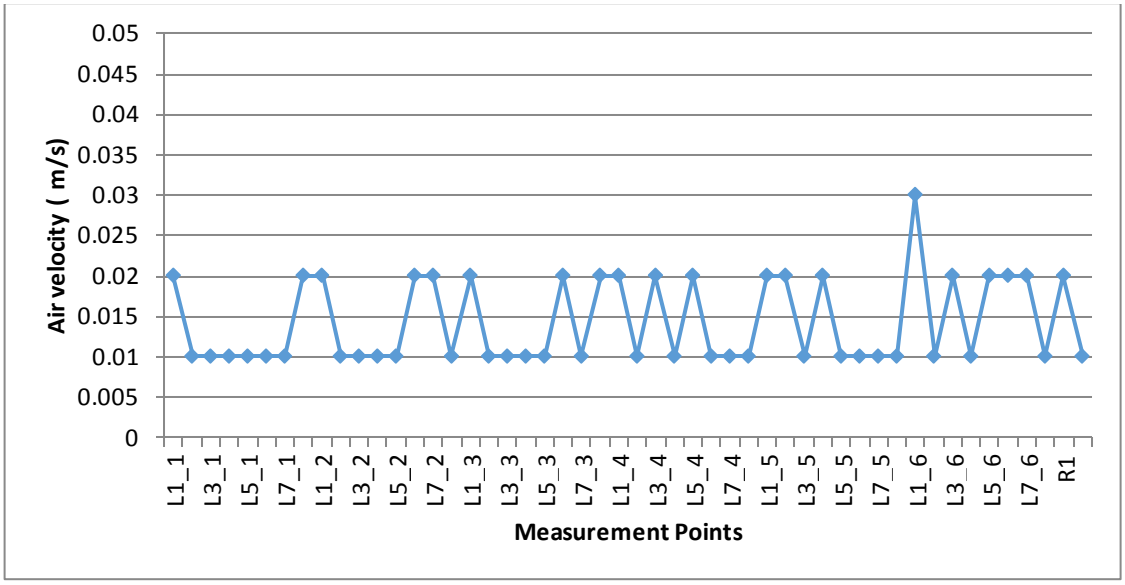

Figure 5.6: Z-axis velocity of measured data.

5.4 CFD modeling

CFD model of the ward tower is shown in Figure 5.7. The building's window is modeled as wall to simplify the modeling process. Adjacent to the ward tower is a 3 storey hospital building.

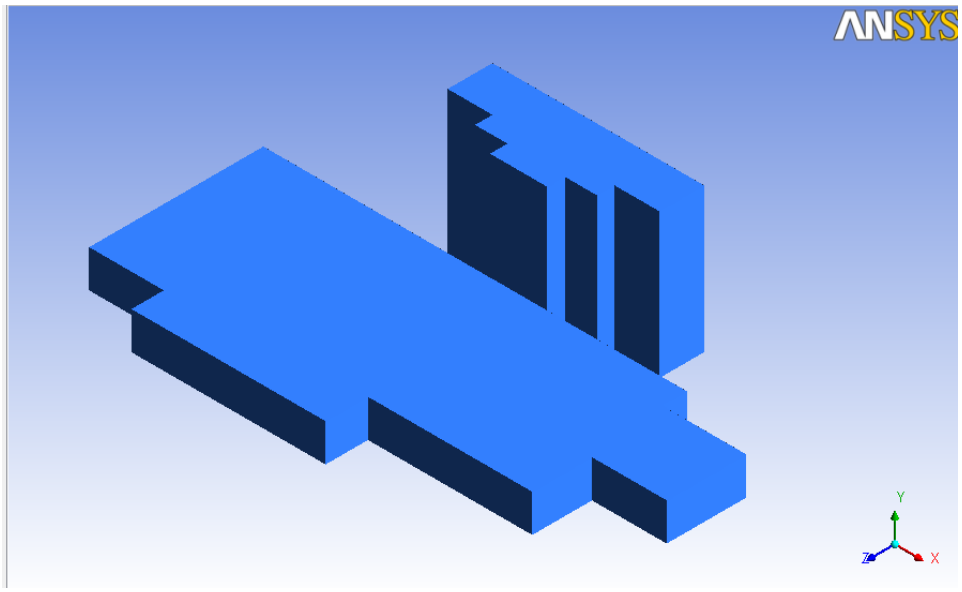

Figure 5.7: CFD model of hospital ward tower.

5.4.1 Domain

This building is located at the middle of domain with lateral and top boundary is set as 5H, inlet boundary is set as 5H and outlet boundary is set as 10H away from building, where H is height of building. This domain is 11H in width, 16H in length and 6H in height, which is 627x912x342m^3, as shown in Figure 5.8. The blockage of this domain is less than suggested 3% blockage ratio.

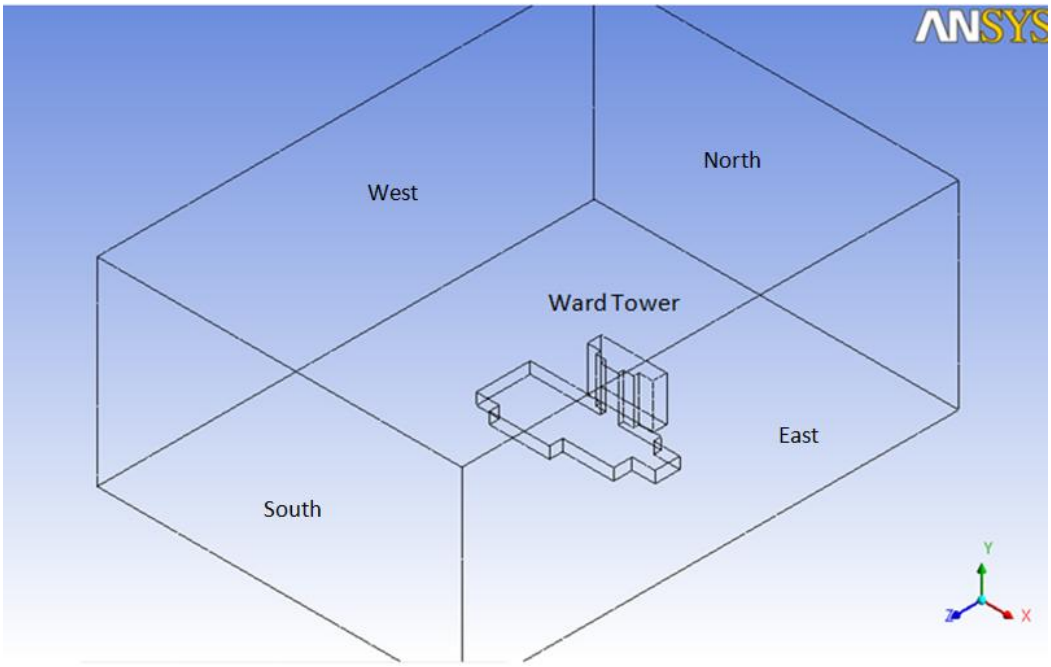

Figure 5.8: Simulation domain.

5.4.2 Boundary Condition

Boundary condition of the CFD simulation is shown in Table 5.1

Table 5.1: Boundary Condition.

Item	Details
Wind inlet	Applied only for Case 2. Velocity at 3ms^{-1} and temperature at 26^{o}C.
Wind outlet	Applied only for Case 2. Pressure outlet was set to zero gauge pressure.

Roof	Set as wall, no-slip condition.
Walls	Set as wall, no-slip condition. The wall is set as 43^{o}C.
Ground	Set as wall, no-slip condition. The ground is set as 46^{o}C

5.4.3 Setting of the simulation

Simulation settings are shown in Table 5.2.

Table 5.2: Simulation setting.

Solver	**Pressure based coupled solver and steady state**
Model	k-Ɛ model, $\sigma_k = 1.0$, $\sigma_e = 1.3$, $C_{1e} = 1.33$ $C_{2e} = 1.92$, $C_\mu = 0.09$ Full buoyancy effects is on to include buoyancy effects on ε. Standard wall treatments.
Solution method	Scheme : SIMPLE Gradient : Least- square cell based Pressure : Standard Momentum : 2^{nd} order upwind Turbulent kinetic energy : 2^{nd} order upwind Turbulent dissipation rate : 2^{nd} order upwind Energy : 2^{nd} order upwind
Solution Control	Under relaxation factor Pressure : 0.3 Density : 1 Body forces :1 Momentum :0.7 Turbulent kinetic energy: 0.8 Turbulent dissipation rate : 0.8 Turbulent viscosity : 0.5 Energy: 1
Convergence criterion	Continuity, x,y,z-velocity, k, epsilon : 5×10^{-4} Energy : 1×10^{-7}

5.5 Mesh independence

For grid independent study, 5 different numbers of meshing element were examined. The number of elements is corresponding to 100, 80, 60, 40 and 20 in fine relevance center at Workbench meshing setting for simulation I, II, III, IV and V respectively as shown in Table 5.3. Firstly it will be visually examined for velocity profile for each simulation. Similar pattern are found in simulation II, III, IV and V. The air velocity value approaches constant as the number of mesh elements increase. Simulations III, IV and V have nearly constant value of velocity as shown in Figure 5.9. Hence, simulation III with 1.6 million meshing element is adopted as it provides adequate accuracy for the simulation.

Table 5.3: Result for Mesh Independency Test.

Case No.	Number of elements	Representative mesh size, h (m)	Ratio, h(n+1)/h(n)
I	646848	6.71	
II	1064117	5.68	1.18
III	1657472	4.90	1.16
IV	2391562	4.33	1.13
V	3558651	3.80	1.14

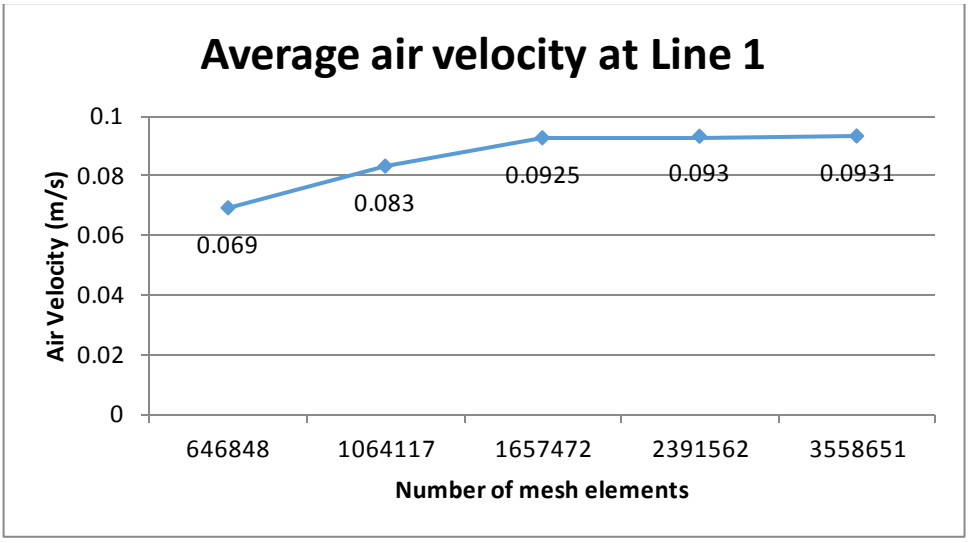

Figure 5.9: Results of grid independency test.

5.6 Verification of model

Figures 5.10 to 5.12 are the comparison between data of physical measurement and simulation for X, Y and Z-axis. The Y-axis for both physical measurement and simulation data is noticed to have similar trend. Overall, X, Y and Z-axis of both data are in good agreement.

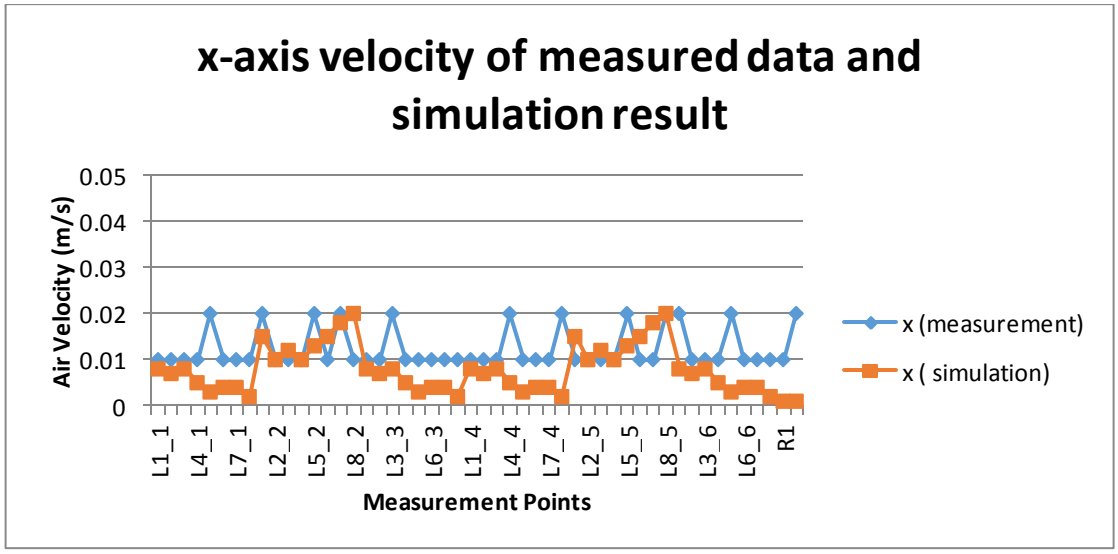

Figure 5.10: X-axis velocity of measured data and simulation result.

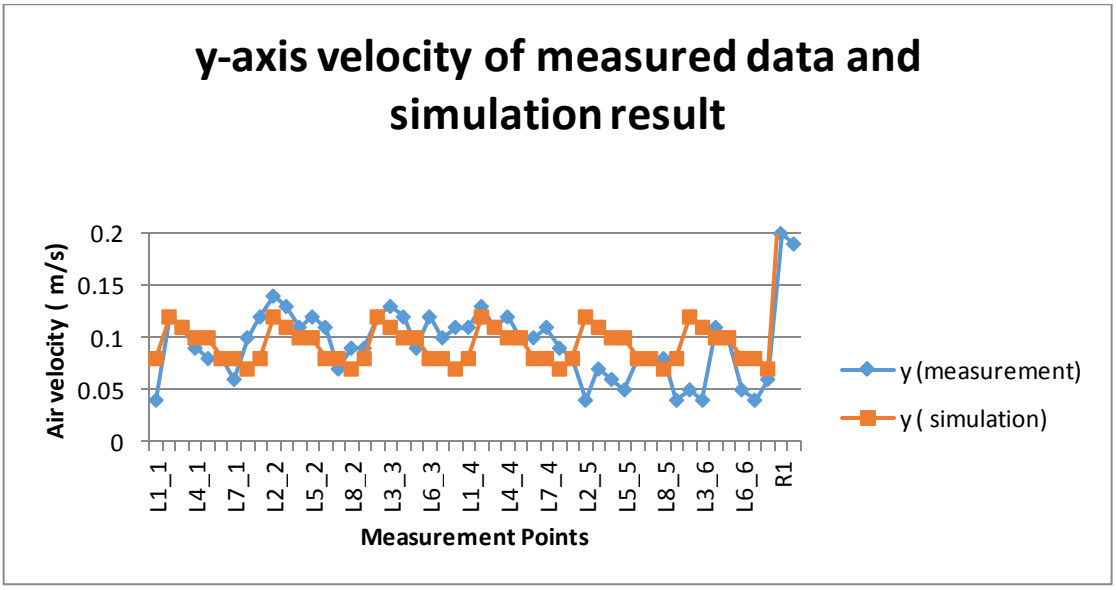

Figure 5.11: Y-axis velocity of measured data and simulation result.

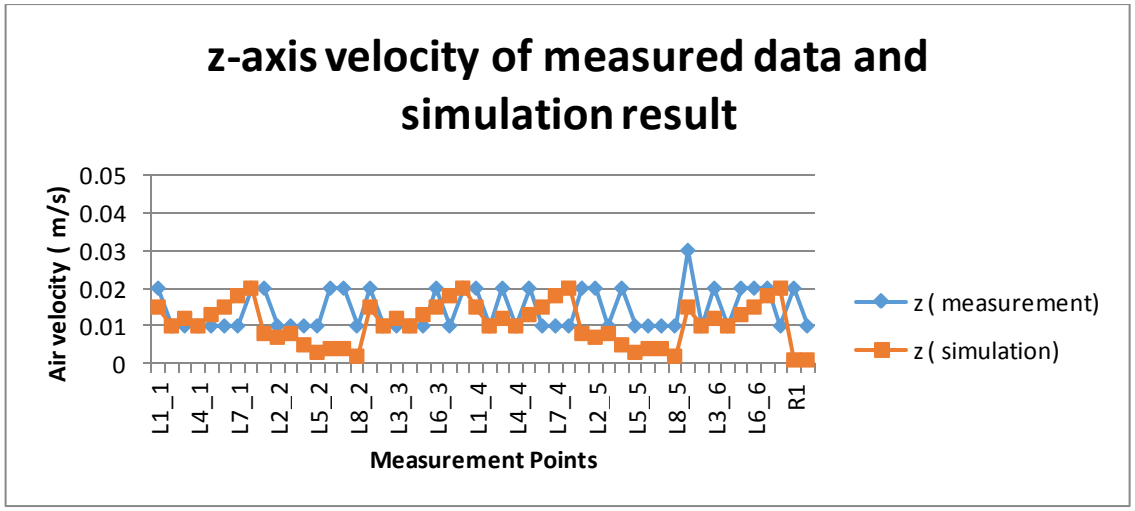

Figure 5.12: Z-axis velocity of measured data and simulation result.

Table 5.4 shows the bias uncertainty analysis of the simulation results with fieldwork measurement. $Average_{max}$ is the average of maximum value between physical and simulation result. $Average_{min}$ is the average of minimum value between physical and simulation result. The bias for maximum value has highest percentage error of 33.3% while

for minimum value has highest percentage of 40%. Due to low average value, slight bias will result in a huge percentage of error, as 0.01ms^{-1} caused 40% of error percentage. The deviation shown is probably due to the assumptions made in the present study.

Table 5.4: Bias Uncertainty.

Axis	$Min_{Physical}$, ms^{-1}	$Min_{Simulation}$, ms^{-1}	Percentage of error, %	$Max_{Physical}$, ms^{-1}	$Max_{Simulation}$, ms^{-1}	Percentage of error,%
X	0.01	0.008	22.2	0.02	0.02	0.0
Y	0.05	0.07	33.3	0.2	0.27	29.8
Z	0.01	0.008	22.2	0.03	0.02	40.0

5.7 CFD simulation result of building

In the discussion, there are three planes had been defined in order to ensure lucidness on the comparison made. Plane YZ (side view) located at the middle of model domain, while plane XZ (top view) is a horizontal plane located at half of the building height.

5.7.1 Case 1

Case 1 is the actual condition with non-windy environment. Figure 5.13 and 5.14 showed the simulation result at YZ (side view) and XY (top view) plane. It can be seen that the airflow is flowing upwards start from the ground along the building. The figure shown adjacent airflow is drawn towards the upward flow as well. The air flow induced by buoyancy has the highest value of 0.15ms^{-1}. Gr/Re^2 has value of 2.14, indicating the flow is dominating by buoyancy effect.

Building surface temperature is higher than ambient temperature, so the air adjacent to building surface will flow upwards from the ground. As ground surface temperature is

higher than building surface temperature, the air flow rise upwards and join the flow that induce by building surface. At the edge of top roof the air velocity is highest due to the force drawn towards the top of the roof.

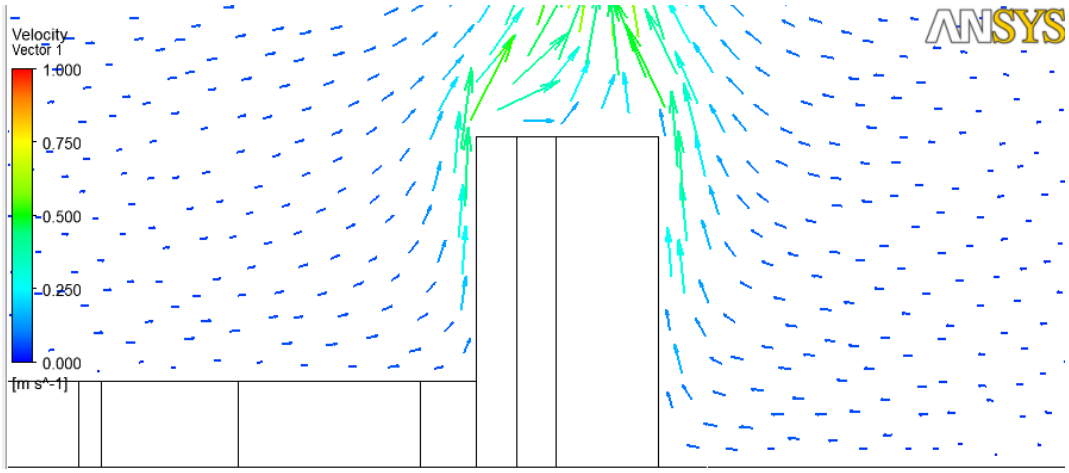

Figure 5.13: YZ plane of simulation result.

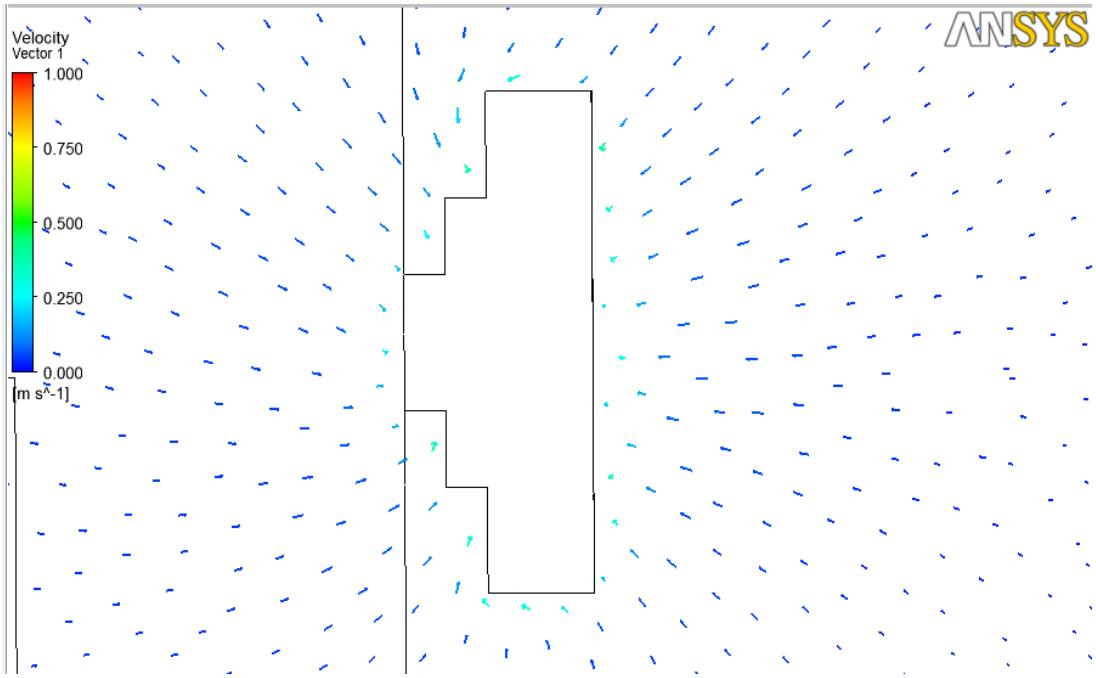

Figure 5.14: XZ plane of simulation result.

5.7.2 Case 2

Case 2 is the simulation of windy environment. Figures 15.15 and 15.16 are the simulation results for Case 2 at YZ (side view) and XZ (top view) plane. It can be seen that the air flow is dominated by the wind direction. The buoyancy effect is insignificant in current airflow. The airflow velocity around the building has highest value of 2.56ms^{-1}. Gr/Re^2 has value of 0.09. This value is much smaller than 1 indicating the air flow is dominating by wind flow.

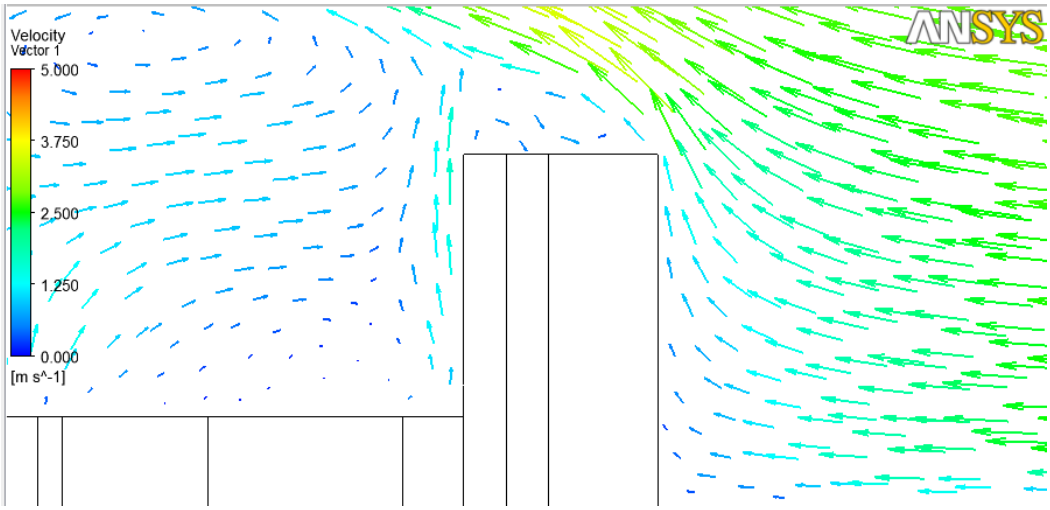

Figure 5.15: YZ plane of simulation result (side view).

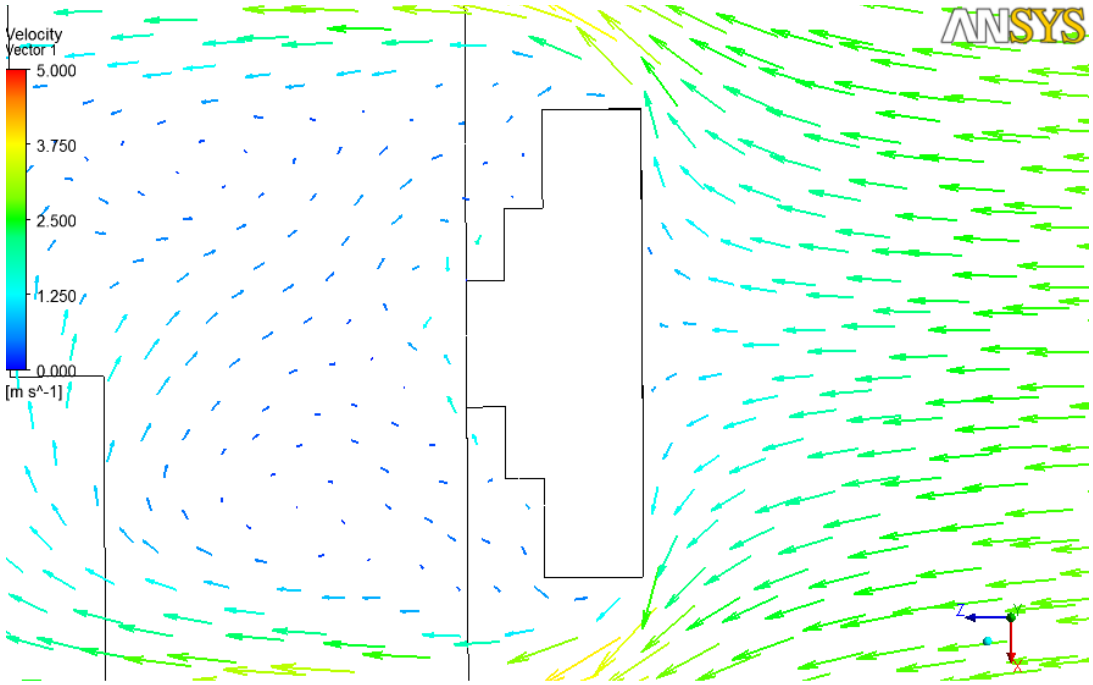

Figure 5.16: XZ plane of simulation result (top view).

5.8 Effect of temperature difference

It is known that air thermal buoyancy is induced due to temperature difference from surrounding. Following simulation is done to study the effect of surface temperature different between ground and building to air velocity induced by buoyancy. Three simulations are carried out under no wind condition. The condition varied for each case is the temperature of ground surface. There are three sets of ground surface temperature, 319K, 329K and 309K. The actual condition of ground surface temperature is 319 K as in Case 1. Figures 5.17 to 5.19 are the graph of air velocity at a vertical line 1 m away from north building surface.

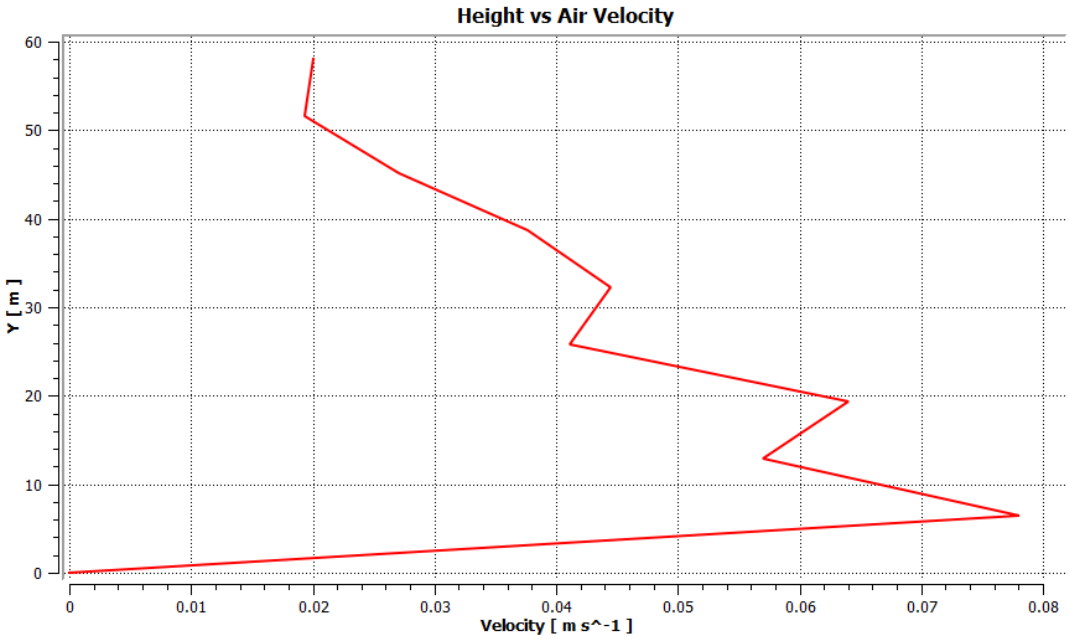

Figure 5.17: Air velocity induced by ground surface temperature of 319K

For ground surface temperature of 319K, the air velocity pattern is shown in Figure 5.17. The air has highest velocity at the bottom region and decreasing when it goes up. The highest air velocity has the value of 0.078ms^{-1}. Ground has higher surface temperature compared to building. So the air velocity induced is higher at the bottom region compared to top region. When it goes up, the air velocity is decreasing.

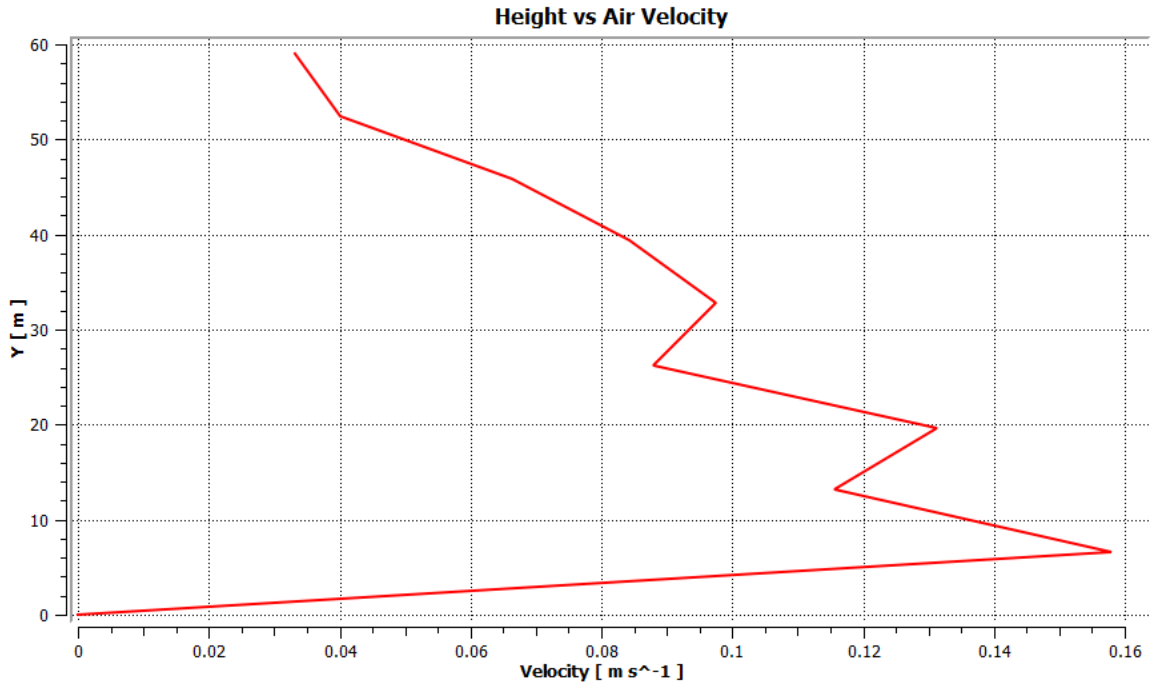

Figure 5.18: Air velocity induced by ground surface temperature of 329K

For ground surface temperature of 329K, the air velocity is shown in Figure 5.18. The air velocity profile is similar to previous condition. It has highest air velocity at bottom region and as it goes up, the air velocity decreases. The highest air velocity induced is 0.158 ms^{-1}. Ground surface temperature is higher than building surface temperature. So region adjacent of ground surface tend to have higher air velocity induced with higher buoyancy effect.

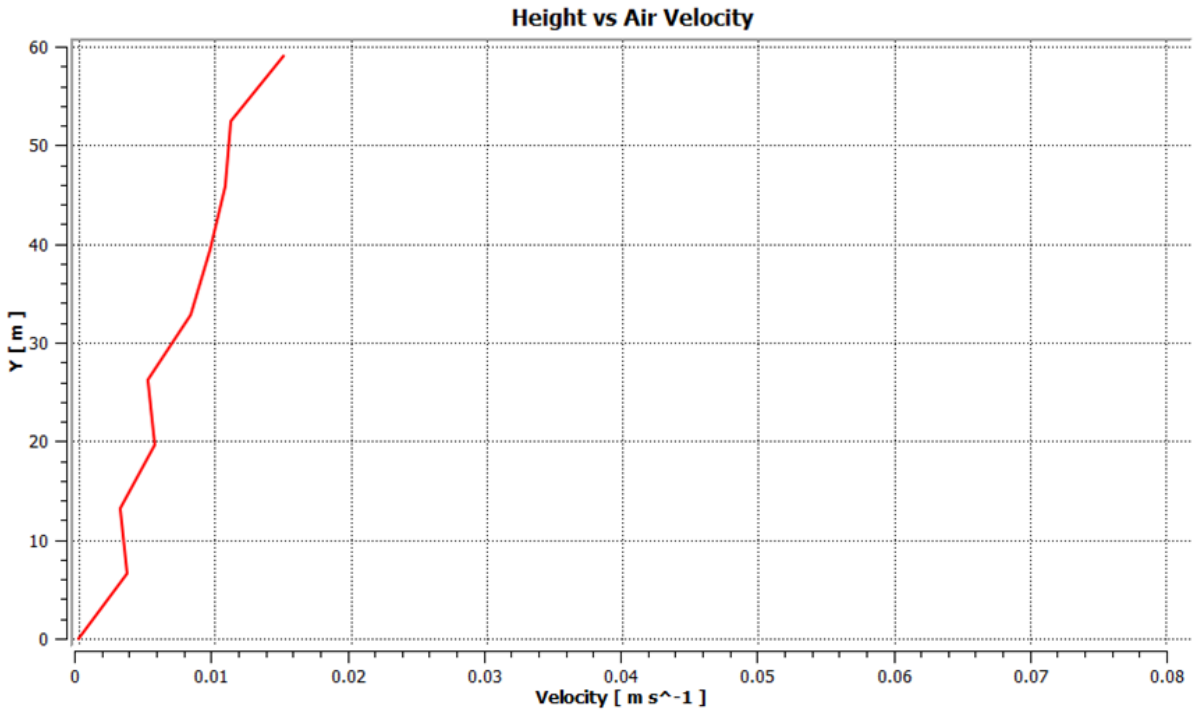

Figure 5.19: Air velocity induced by ground surface temperature of 309K.

Figure 5.19 is the air velocity induced by ground surface temperature of 309K. The bottom has lower air velocity and increasing when height goes up with highest air velocity is 0.015ms^{-1}.Region adjacent to ground has lower surface temperature compare to region adjacent to building surface. So at the bottom region, the air velocity induced is lower as buoyancy effect is smaller compare to top upper region. So the air tend to move slowly compare to the upper region.

From these three simulations, the range of air velocity at the top region is from 0.015 to 0.035 ms^{-1} while at the bottom region from 0.004 to 0.158ms^{-1}.

5.9 Concluding summary

In this chapter, two different investigations are carried out. First investigation is to study the buoyancy effect to air flow surrounding a hospital ward tower with and without present of wind. Second investigation studied the effect of temperature difference of ground surface to air velocity induced.

- Buoyancy effect does not bring significant effect on airflow in the present of wind as the airflow is dominating by wind direction. However, if the wind is not present, the air is flowing vertically upwards, which is induced by buoyancy effect.
- Magnitude of air velocity induced by buoyancy is affected by the temperature difference from surrounding surface. The greater temperature difference, the greater magnitude of air velocity induced.

CHAPTER 6

CASE STUDY OF ENGINEERING TOWER

6.0 Case Study of Engineering Tower

6.1 Overview

Engineering Tower in Engineering Faculty of University Malaya is a 8-stroreys building as shown in Figure 6.1. Engineering Tower is denoted as Block L which it is surrounding by other building. The plan view of Engineering Tower is shown in Figure 6.2. This building has conventional shape similar with ward tower building (Chapter 5). Hence similar methodology is adopted in this case study.

Figure 6.1: Engineering Tower.

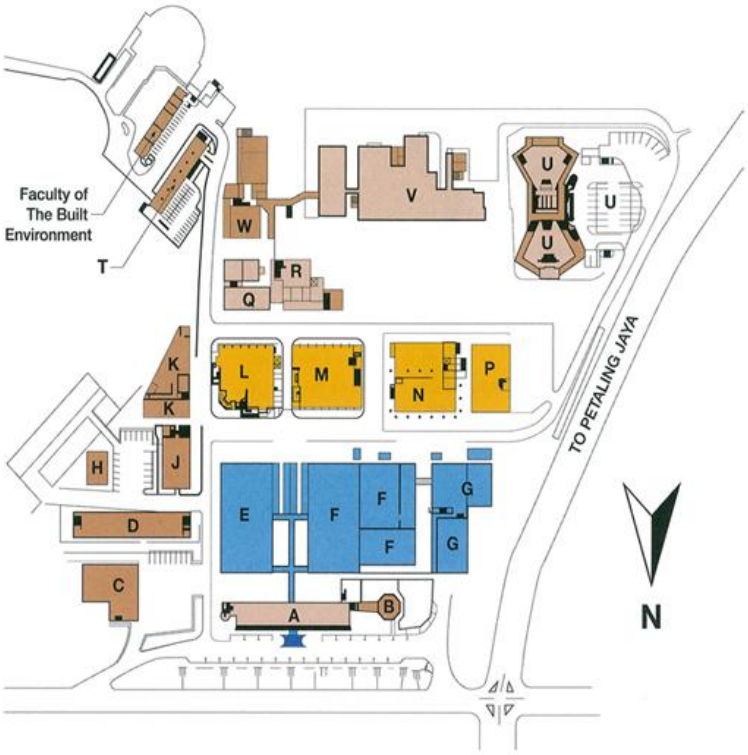

Figure 6.2: Site Map of Engineering Tower, Block L.

6.2 Measurement of Building

The measurement is taken for 1month from 25 February to 29March 2013. There are 19 measurement points. The parameters taken such as the surface temperature, ambient air temperature and wind speed.

6.3 Physical measurement

The physical measurement data is plotted in graph as in Figures 6.3- 6.5. From figure, it is noticed that the X and Z-axis velocity is very low compared to Y-axis velocity. This is due to buoyancy effect is contributed to only Y-axis of velocity.

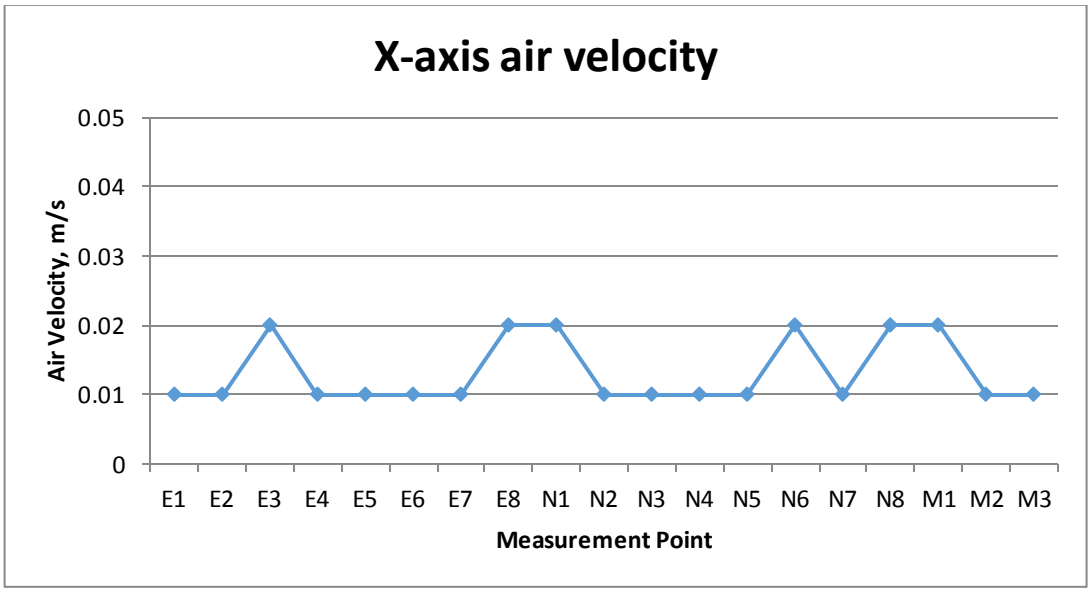

Figure 6.3: X-axis air velocity.

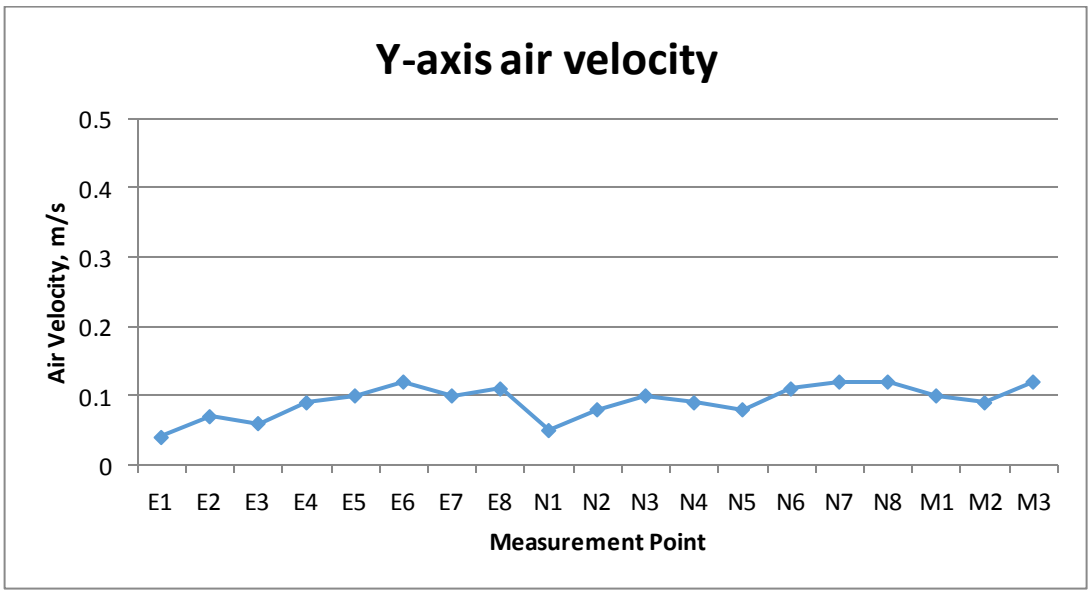

Figure 6.4: Y-axis air velocity.

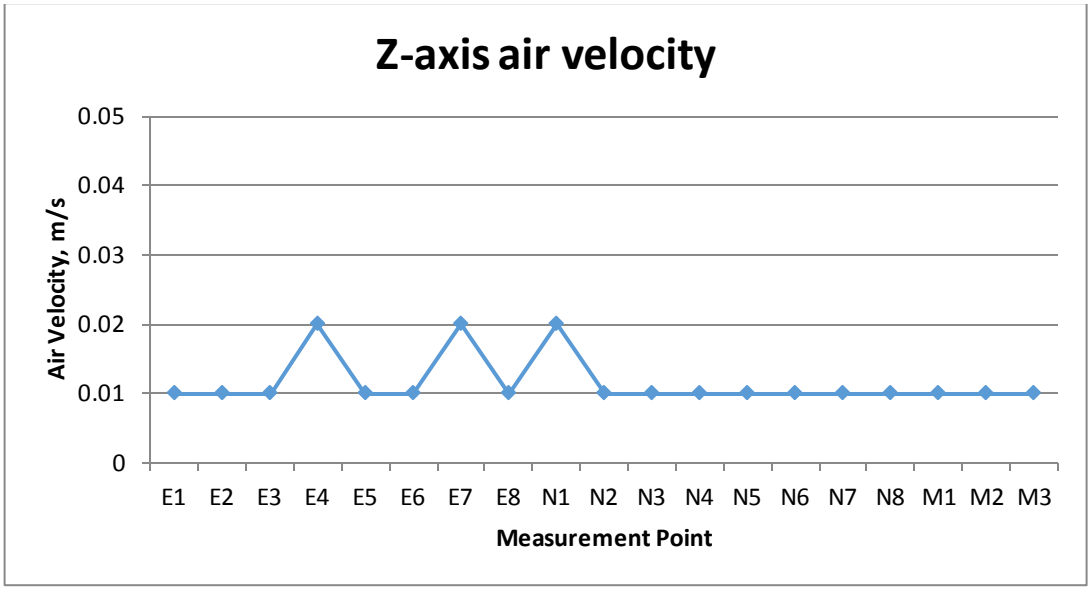

Figure 6.5: Z-axis air velocity.

6.4 CFD Modeling

The CFD modeling method is same as Chapter 5.

6.5 Mesh independence

Same mesh independence method as Chapter 5 is adopted. Detail of Simulation I, II, III, IV and V are shown in Table 6.1. Similar pattern are found in simulation II, III, IV and V. The velocity at Line 1 from different mesh elements are plotted in graphs shown in Figure 6.6. Line 1 is a vertical line located 1m away from the building surface. The air velocity value approaches constant as the number of mesh increases. Simulation IV and V have a constant value of air velocity. Hence, simulation IV with 2.3 million meshing elements is adopted as no further deviation of air velocity with increasing meshing element afterwards.

Table 6.1: Mesh Independence Test Detail.

Case No.	Number of elements	Representative mesh size, h (m)	Ratio, h(n+1)/h(n)
I	571354	8.43	
II	984602	7.31	1.15
III	1657472	6.47	1.13
IV	2307485	5.62	1.15
V	2986149	4.43	1.19

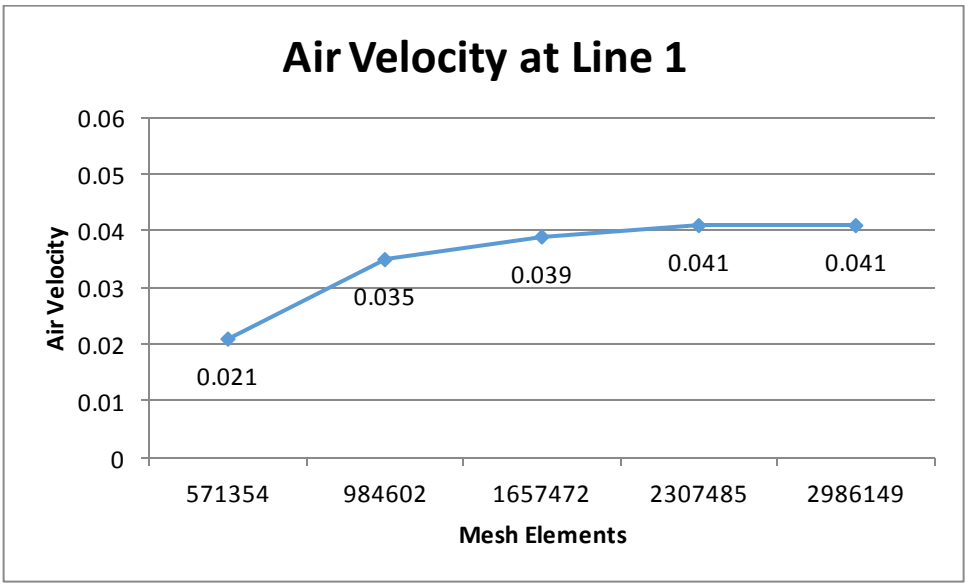

Figure 6.6: Result of grid independency test.

6.6 Verification of model

Figures 6.7 to 6.9 is the comparison between data of physical measurement and simulation for X, Y and Z axis. The Y-axis for both physical measurement and simulation data is noticed to have similar trend which Y-axis is the buoyancy induced direction. X and Z axis air velocity comparison has shown slight deviation as simulation data laid below physical data.

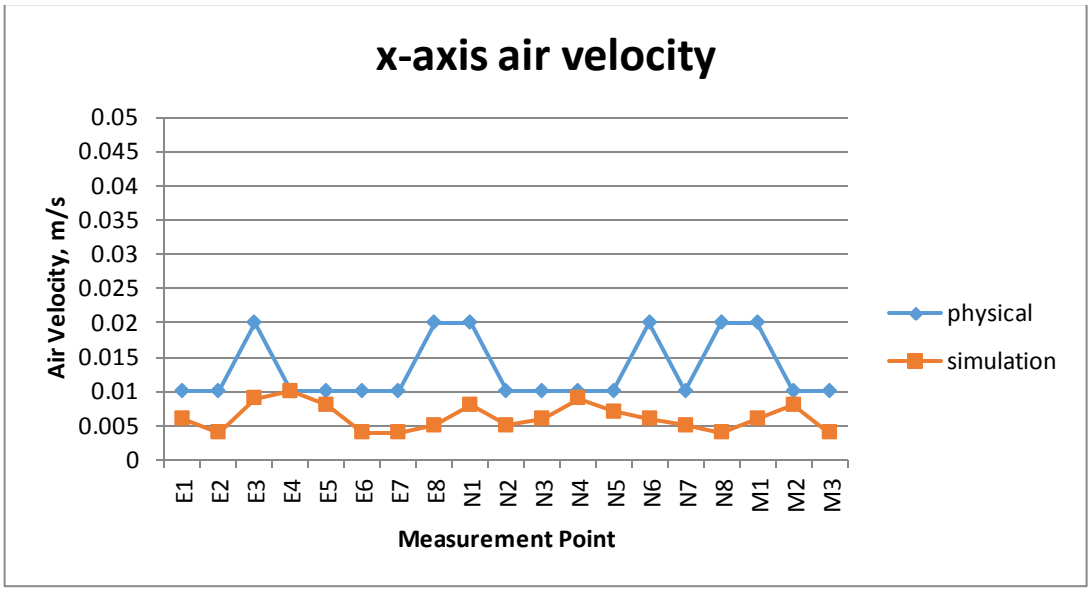

Figure 6.7: X-axis velocity of measured data and simulation result.

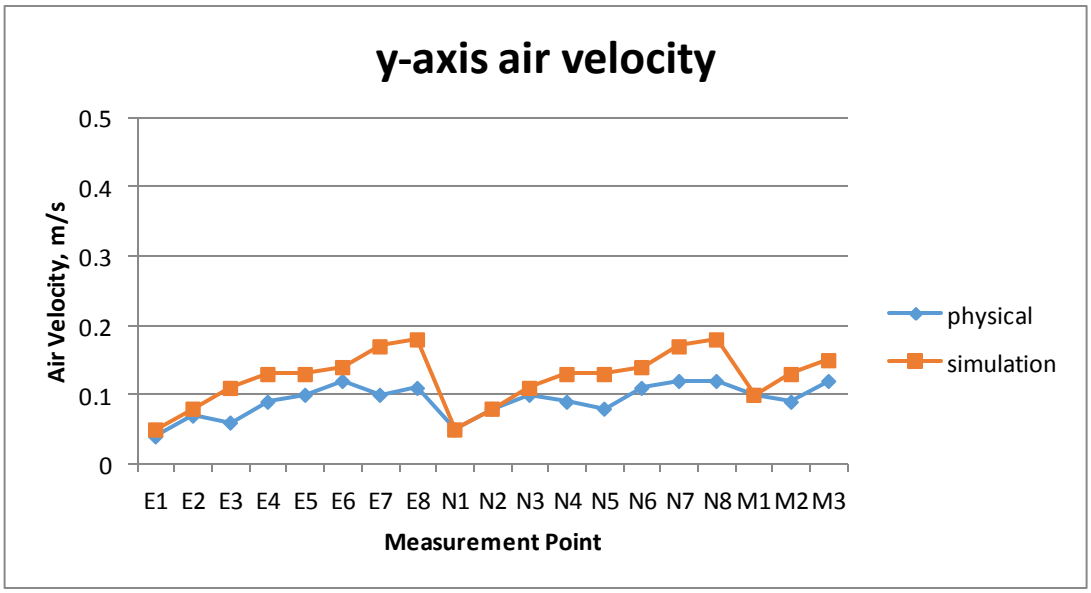

Figure 6.8: Y-axis velocity of measured data and simulation result.

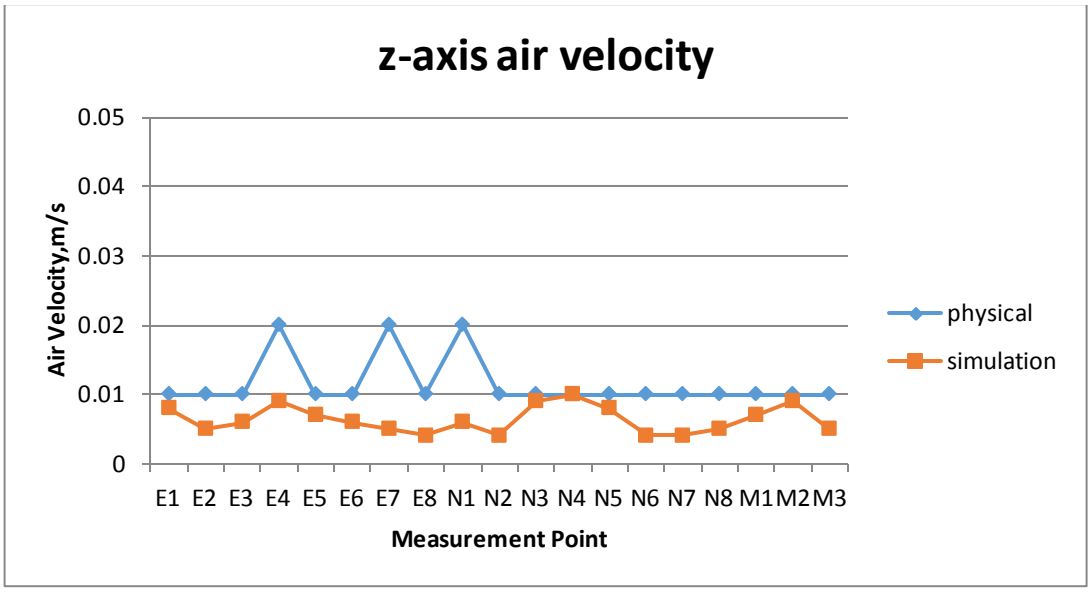

Figure 6.9: Z-axis velocity of measured data and simulation result.

Table 6.2 shows the bias uncertainty analysis of the simulation results with fieldwork measurement. The bias for maximum value has highest percentage error of 60 while for minimum value has highest percentage of of 57.1%. Due to low average value, slight bias will result in a huge percentage of error. Y-axis air velocity has lowest percentages error compared to x and z component of air velocity. The deviation shown is probably due to the assumptions made in the present study.

Table 6.2: Bias Uncertainty.

Axis	$Min_{Physical}$, ms^{-1}	$Min_{Simulation}$, ms^{-1}	Percentage of error, %	$Max_{Physical}$, ms^{-1}	$Max_{Simulation}$, ms^{-1}	Percentage of error,%
X	0.01	0.004	57.1	0.02	0.01	60.0
Y	0.04	0.050	22.2	0.12	0.18	32.1
Z	0.01	0.004	57.1	0.02	0.01	60.0

6.7 CFD result

Figure 6.10 is the CFD result. This simulation is carried out under no wind condition. As in actual condition, Engineering Tower is surrounded by other buildings, the outdoor environment is non-windy during the physical measurement. The air flow is rising from the bottom towards the top of the building which is induced by buoyancy effect. Figure 6.11 showed the air flow velocity profile at 0.5m away from building façade. Air velocity is increasing from bottom to top. This is due to ground temperature is slight cooler than building surface temperature, which has been discussed in Chapter 5. The ground surface temperature is cooler is caused by shading from surrounding.

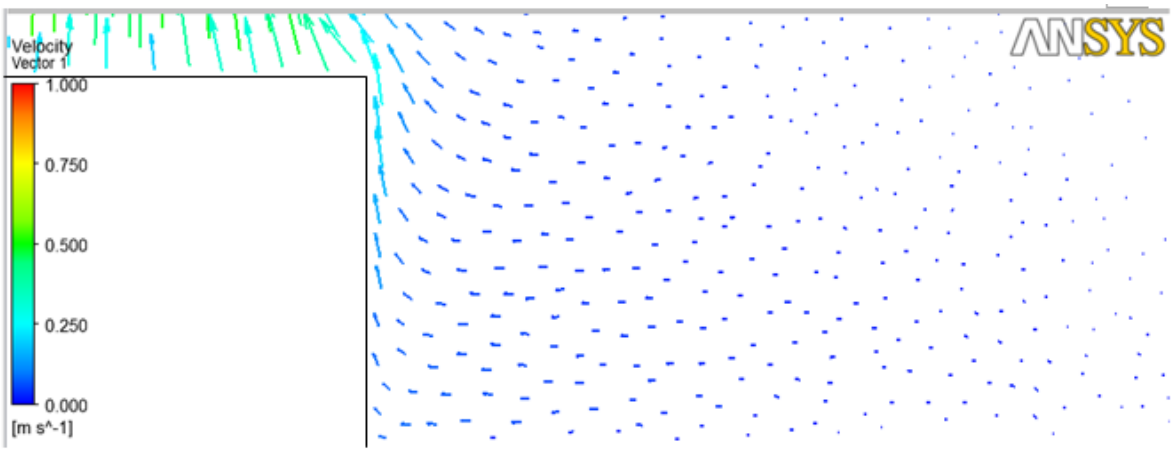

Figure 6.10: Simulation result (side view)

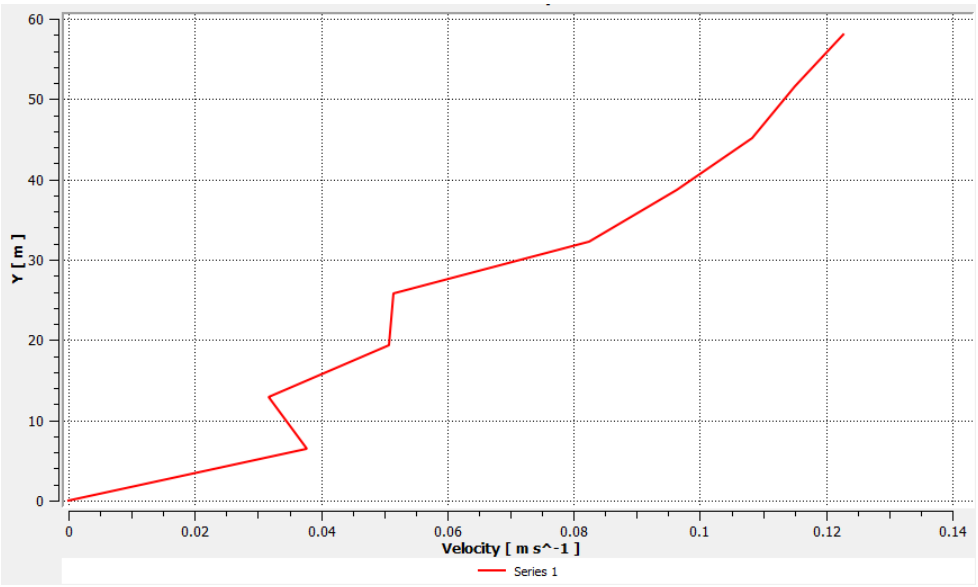

Figure 6.11: Air velocity profile.

6.8 Concluding summary

In this chapter, investigations are carried out to study the buoyancy effect to air flow surrounding Engineering Tower of University Malaya.

- Buoyancy effect induced the air flow surrounding the building. The value of air velocity induced increasing from the bottom to the top of building, which same as the discussion in Chapter 5.

CHAPTER 7

CONCLUSION AND RECOMMENDATIONS

7.0 Conclusion and Recommendations

Air flow surrounding building has been an important issue when designing building envelope. Air flow has been widely studied to investigate the effect to buildings, which has been developed to natural ventilation. Hence, effect of buoyancy towards air flow is studied. In this research, green building and conventional building are studied. Two main points can be concluded.

First conclusion, buoyancy did affect the air flow movement under circumstances of non-windy environment. With windy environment, air flow movement is dominating by wind force and buoyancy effect is insignificant.

Second conclusion, temperature difference among building and ground surface affects magnitude of air velocity induced. The greater the temperature difference, the greater the air velocity induced by buoyancy effect.

The just mentioned results can serve as a valuable guide to M&E design engineers and professional architects in designing tropical green building ACMV systems and building facades in the future.

Nevertheless, there are some shortcomings in the present research knowing that the outdoor environments are hardly predictable and constant. Despite the imperfections, the present study has given a significant new insight in the thermal effect to buildings in the tropics and has illustrated the effect of the buoyancy to the airflow.

References

Abd Razak, Azli, Hagishima, Aya, Ikegaya, Naoki, & Tanimoto, Jun. (2013). Analysis of airflow over building arrays for assessment of urban wind environment. *Building and Environment,* **59**, 56-65.

Ahmed, Khandaker Shabbir. (2003). Comfort in urban spaces: defining the boundaries of outdoor thermal comfort for the tropical urban environments. *Energy and Buildings,* **35**(1), 103-110.

AIAA. (1998). Guide for the verification and validation of computational fluid dynamics simulations. AIAA Standard G-077-1998. American Institute of Aeronautics and Astronautics, Reston, VA.

Al-Sallal, Khaled A., & Al-Rais, Laila. (2012). Outdoor airflow analysis and potential for passive cooling in the modern urban context of Dubai. *Renewable Energy,* **38**(1), 40-49.

An, K., Fung, J. C. H., & Yim, S. H. L. (2013). Sensitivity of inflow boundary conditions on downstream wind and turbulence profiles through building obstacles using a CFD approach. *Journal of Wind Engineering and Industrial Aerodynamics,* **115**, 137-149.

ANSYS. (2009a). ANSYS FLUENT 12.0 User's guide. Canonsburg, Pennsylvania: ANSYS Inc.

ANSYS. (2009b). ANSYS Workbench User's Guide.

Arce, J., Jiménez, M. J., Guzmán, J. D., Heras, M. R., Alvarez, G., & Xamán, J. (2009). Experimental study for natural ventilation on a solar chimney. *Renewable Energy,* **34**(12), 2928-2934.

Assimakopoulos, V. D., Georgakis, C., & Santamouris, M. (2006). Experimental validation of a computational fluid dynamics code to predict the wind speed in street canyons for passive cooling purposes. *Solar Energy,* **80**(4), 423-434.

Bauer, Michael, Mösle, Peter, & Schwarz, Michael. (2009). *Green building: Guidebook for sustainable architecture*: Springer.

Blocken, B., Janssen, W. D., & van Hooff, T. (2012). CFD simulation for pedestrian wind comfort and wind safety in urban areas: General decision framework and case study for the Eindhoven University campus. *Environmental Modelling & Software,* **30**, 15-34.

Blocken, B., Stathopoulos, Ted, & Carmeliet, Jan. (2007). CFD simulation of the atmospheric boundary layer: wall function problems. *Atmospheric Environment,* **41**(2), 238-252.

Blocken, B, Stathopoulos, T, Saathoff, P, & Wang, X. (2008). Numerical evaluation of pollutant dispersion in the built environment: comparisons between models and experiments. *Journal of Wind Engineering and Industrial Aerodynamics,* **96**(10), 1817-1831.

Bourbia, F., & Awbi, H. B. (2004). Building cluster and shading in urban canyon for hot dry climate. *Renewable Energy,* **29**(2), 249-262.

Bourbia, F., & Boucheriba, F. (2010). Impact of street design on urban microclimate for semi arid climate (Constantine). *Renewable Energy,* **35**(2), 343-347.

Chang, Kuei-Feng, & Chou, Po-Cheng. (2010). Measuring the influence of the greening design of the building environment on the urban real estate market in Taiwan. *Building and Environment,* **45**(10), 2057-2067.

Chen, Q. (2009). Ventilation performance prediction for buildings: A method overview and recent applications. *Building and Environment,* **44**(4), 848-858.

Coussirat, M., Guardo, A., Jou, E., Egusquiza, E., Cuerva, E., & Alavedra, P. (2008). Performance and influence of numerical sub-models on the CFD simulation of free and forced convection in double-glazed ventilated façades. *Energy and Buildings,* **40**(10), 1781-1789.

Eliasson, I., Offerle, B., Grimmond, C. S. B., & Lindqvist, S. (2006). Wind fields and turbulence statistics in an urban street canyon. *Atmospheric Environment,* **40**(1), 1-16.

Fahmy, Mohamad, & Sharples, Stephen. (2009). On the development of an urban passive thermal comfort system in Cairo, Egypt. *Building and Environment,* **44**(9), 1907-1916.

Franke, Jorg, Hellsten, Antti, Schlunzen, K Heinke, & Carissimo, Bertrand. (2011). The COST 732 Best Practice Guideline for CFD simulation of flows in the urban environment: a summary. *International Journal of Environment and Pollution,* **44**(1), 419-427.

Gao, Y., & Chow, W. K. (2005). Numerical studies on air flow around a cube. *Journal of Wind Engineering and Industrial Aerodynamics,* **93**(2), 115-135.

Garde-Bentaleb, F, Miranville, F, Boyer, H, & Depecker, P. (2002). Bringing scientific knowledge from research to the professional fields: the case of the thermal and airflow design of buildings in tropical climates. *Energy and Buildings,* **34**(5), 511-521.

Georgakis, Ch, & Santamouris, M. (2006). Experimental investigation of air flow and temperature distribution in deep urban canyons for natural ventilation purposes. *Energy and Buildings,* **38**(4), 367-376.

Givoni, Baruch, Noguchi, Mikiko, Saaroni, Hadas, Pochter, Oded, Yaacov, Yaron, Feller, Noa, & Becker, Stefan. (2003). Outdoor comfort research issues. *Energy and Buildings,* **35**(1), 77-86.

Hargreaves, D. M., & Wright, N. G. (2007). On the use of the k– model in commercial CFD software to model the neutral atmospheric boundary layer. *Journal of Wind Engineering and Industrial Aerodynamics,* **95**(5), 355-369.

Hew, ZX, & Rap, SP. (2012). Active energy conserving strategies of the Malaysia Energy Commision Diamond Building. *Sustainable Future for Human Security (SUSTAIN).*

Hooff, T. van, & Blocken, B. (2010). On the effect of wind direction and urban surroundings on natural ventilation of a large semi-enclosed stadium. *Computers & Fluids,* **39**(7), 1146-1155.

Huovila, Pekka. (2007). *Buildings and climate change: status, challenges, and opportunities*: UNEP/Earthprint.

Jiang, Dehai, Jiang, Weimei, Liu, Hongnian, & Sun, Jianning. (2008). Systematic influence of different building spacing, height and layout on mean wind and turbulent characteristics within and over urban building arrays. *Wind and Structures,* **11**(4), 275-289.

Johansson, Erik, Thorsson, Sofia, Emmanuel, Rohinton, & Krüger, Eduardo. (2014). Instruments and methods in outdoor thermal comfort studies – The need for standardization. *Urban Climate*.

Kitous, Samia, Bensalem, Rafik, & Adolphe, Luc. (2012). Airflow patterns within a complex urban topography under hot and dry climate in the Algerian Sahara. *Building and Environment*, **56**, 162-175.

Lu, Jun, Chen, Jin-hua, Tang, Ying, & Wang, Jin-sha. (2007). High-Rise Buildings versus Outdoor Thermal Environment in Chongqing. *Sensors*, **7**(10), 2183-2200.

Makaremi, Nastaran, Salleh, Elias, Jaafar, Mohammad Zaky, & GhaffarianHoseini, AmirHosein. (2012). Thermal comfort conditions of shaded outdoor spaces in hot and humid climate of Malaysia. *Building and environment*, **48**, 7-14.

Malmqvist, Tove, & Glaumann, Mauritz. (2009). Environmental efficiency in residential buildings–A simplified communication approach. *Building and Environment*, **44**(5), 937-947.

Masnavi, MR. (2007). Measuring urban sustainability: Developing a conceptual framework for bridging the gap between theoretical levels and the operational levels.

Memarzadeh, Farhad, & Jiang, J. (2010). Effect of operation room geometry and ventilation system parameter variations on the protection of the surgical site.

Morakinyo, Tobi Eniolu, Balogun, Ahmed Adedoyin, & Adegun, Olumuyiwa Bayode. (2013). Comparing the effect of trees on thermal conditions of two typical urban buildings. *Urban Climate*, **3**, 76-93.

Nakamura, Y, & Oke, TR. (1988). Wind, temperature and stability conditions in an east-west oriented urban canyon. *Atmospheric Environment (1967)*, **22**(12), 2691-2700.

Niachou, K., Livada, I., & Santamouris, M. (2008a). Experimental study of temperature and airflow distribution inside an urban street canyon during hot summer weather conditions—Part I: Air and surface temperatures. *Building and Environment*, **43**(8), 1383-1392.

Niachou, K., Livada, I., & Santamouris, M. (2008b). Experimental study of temperature and airflow distribution inside an urban street canyon during hot summer weather conditions. Part II: Airflow analysis. *Building and Environment*, **43**(8), 1393-1403.

Oberkampf, William L, & Trucano, Timothy G. (2002). Verification and validation in computational fluid dynamics. *Progress in Aerospace Sciences*, **38**(3), 209-272.

Oke, Tim R. (1973). City size and the urban heat island. *Atmospheric Environment (1967)*, **7**(8), 769-779.

Oke, Tim R. (1982). The energetic basis of the urban heat island. *Quarterly Journal of the Royal Meteorological Society*, **108**(455), 1-24.

Perini, Katia, Ottelé, Marc, Fraaij, ALA, Haas, EM, & Raiteri, Rossana. (2011). Vertical greening systems and the effect on air flow and temperature on the building envelope. *Building and Environment*, **46**(11), 2287-2294.

Rajapaksha, I., Nagai, H., & Okumiya, M. (2003). A ventilated courtyard as a passive cooling strategy in the warm humid tropics. *Renewable Energy*, **28**(11), 1755-1778.

Rizk, Ahmed A., & Henze, Gregor P. (2010). Improved airflow around multiple rows of buildings in hot arid climates. *Energy and Buildings*, **42**(10), 1711-1718.

Rohdin, P., & Moshfegh, B. (2007). Numerical predictions of indoor climate in large industrial premises. A comparison between different k–ε models supported by field measurements. *Building and Environment*, **42**(11), 3872-3882.

Rosenzweig, Cynthia, Solecki, William D, Parshall, Lily, Chopping, Mark, Pope, Gregory, & Goldberg, Richard. (2005). Characterizing the urban heat island in current and future climates in New Jersey. *Global Environmental Change Part B: Environmental Hazards*, **6**(1), 51-62.

Sanusi, Aliyah N. Z., Shao, Li, & Ibrahim, Najib. (2013). Passive ground cooling system for low energy buildings in Malaysia (hot and humid climates). *Renewable Energy*, **49**, 193-196.

Shahidan, Mohd Fairuz, Jones, Phillip J, Gwilliam, Julie, & Salleh, Elias. (2012). An evaluation of outdoor and building environment cooling achieved through combination modification of trees with ground materials. *Building and Environment*, **58**, 245-257.

Sini, Jean-François, Anquetin, Sandrine, & Mestayer, Patrice G. (1996). Pollutant dispersion and thermal effects in urban street canyons. *Atmospheric environment*, **30**(15), 2659-2677.

Taha, Haider. (1997). Urban climates and heat islands: albedo, evapotranspiration, and anthropogenic heat. *Energy and buildings*, **25**(2), 99-103.

Tang, Li, Nikolopoulou, Marialena, Zhao, Fu-yun, & Zhang, Nan. (2012). CFD modeling of the built environment in Chinese historic settlements. *Energy and Buildings*, **55**, 601-606.

Tanny, Josef, Haslavsky, Vitaly, & Teitel, Meir. (2008). Airflow and heat flux through the vertical opening of buoyancy-induced naturally ventilated enclosures. *Energy and Buildings*, **40**(4), 637-646.

Tominaga, Yoshihide, Mochida, Akashi, Yoshie, Ryuichiro, Kataoka, Hiroto, Nozu, Tsuyoshi, Yoshikawa, Masaru, & Shirasawa, Taichi. (2008). AIJ guidelines for practical applications of CFD to pedestrian wind environment around buildings. *Journal of Wind Engineering and Industrial Aerodynamics*, **96**(10-11), 1749-1761.

Tong, Guohong, Zhang, Guoqiang, Christopher, David M., Bjerg, Bjarne, Ye, Zhangying, & Cheng, Jin. (2013). Evaluation of turbulence models to predict airflow and ammonia concentrations in a scale model swine building enclosure. *Computers & Fluids*, **71**, 240-249.

Tripathi, Brajesh, & Moulic, S. G. (2007). Investigation of the buoyancy affected airflow patterns in the enclosure subjected at the different wall temperatures. *Energy and Buildings*, **39**(8), 906-912.

van Hooff, T., & Blocken, B. (2010). Coupled urban wind flow and indoor natural ventilation modelling on a high-resolution grid: A case study for the Amsterdam ArenA stadium. *Environmental Modelling & Software*, **25**(1), 51-65.

van Hooff, T., & Blocken, B. (2013). CFD evaluation of natural ventilation of indoor environments by the concentration decay method: CO2 gas dispersion from a semi-enclosed stadium. *Building and Environment*, **61**, 1-17.

Van Maele, K,, & Merci, B. (2006). Application of two buoyancy-modified – turbulence models to different types of buoyant plumes. *Fire Safety Journal*, **41**(2), 122-138.

Wieringa, Jon. (1992). Updating the Davenport roughness classification. *Journal of Wind Engineering and Industrial Aerodynamics*, **41**(1), 357-368.

Wong, N. H., Kardinal Jusuf, Steve, Aung La Win, Aung, Kyaw Thu, Htun, Syatia Negara, To, & Xuchao, Wu. (2007). Environmental study of the impact of greenery in an institutional campus in the tropics. *Building and Environment*, **42**(8), 2949-2970.

Zhang, Rui, Zhang, Yongjie, Lam, Khee Poh, & Archer, David H. (2010). A prototype mesh generation tool for CFD simulations in architecture domain. *Building and Environment*, **45**(10), 2253-2262.